For Reference

NOT TO BE TAKEN FROM THIS ROOM

For Reference

NOT TO BE TAKEN FROM THIS ROOM

Ex libris
universitatis
albertaensis

QUAECUMQUE VERA

The University of Alberta
Printing Department
Edmonton, Alberta

[illegible]

[illegible]

[illegible]

[illegible]

© [illegible]

[illegible]

[illegible]

[illegible]

[illegible]

[illegible]

[illegible]

[illegible]

Thesis
1969 (F)
50

THE UNIVERSITY OF ALBERTA

The Crystal Structures of Two Inorganic Compounds

by

© Mary Elisabeth Cradwick

A THESIS

SUBMITTED TO THE FACULTY OF GRADUATE STUDIES

IN PARTIAL FULFILMENT OF THE REQUIREMENTS FOR

THE DEGREE OF MASTER OF SCIENCE

Department of Chemistry

Edmonton, Alberta

Fall, 1969

UNIVERSITY OF ALBERTA
FACULTY OF GRADUATE STUDIES

The undersigned certify that they have read, and recommend to the Faculty of Graduate Studies for acceptance, a thesis entitled THE CRYSTAL STRUCTURES OF TWO INORGANIC COMPOUNDS submitted by Mary Elisabeth Cradwick in partial fulfilment of the requirements for the degree of Master of Science.

TABLE OF CONTENTS

Page

Abstract i

Acknowledgements ii

List of Figures iii

List of Tables iv

The Crystal Structure of 2,2'-bipyridyl(tribromogermanium)μ-bromotricarbonyl tungsten ($bipy(CO)_3BrWGeBr_3$)

Introduction 1

Experimental 8

Structure Determination 11

Results 26

Molecular Geometry 44

Discussion 48

The Crystal Structure of tetraethylamineplatinum II tetrachloroplatinate II ($[Pt(etNH_2)_4][PtC\ell_4]$).

Introduction 52

Experimental 55

Structure Analysis 58

Results 63

Discussion 73

References 79

ABSTRACT

The crystal structure of 2,2'-bipyridyl(tribromogermanium)-μ-bromotricarbonyltungsten (bipy(CO)$_3$BrWGeBr$_3$) has been determined in order to establish the co-ordination geometry of the heptaco-ordinate tungsten atom. This is found to approximate to a capped trigonal prism with a bromine atom (attached to the tungsten atom) lying above the centre of one of the square faces formed by the germanium atom, the two nitrogen atoms of the bipyridyl ligand and a carbonyl group.

The crystal structure of tetraethylamineplatinum II tetrachloroplatinate II ([Pt(etNH$_2$)$_4$][PtCℓ$_4$]) shows it to consist of parallel chains of alternating cations and anions in which the distance between adjacent platinum atoms is 3.62 Å. This structure, while essentially similar to that of Magnus' green salt ([Pt(NH$_3$)$_4$][PtCℓ$_4$]), differs in the mutual orientation of the anion and cation co-ordination plane; these are not parallel (dihedral angle of 151°) as was observed for Magnus' green salt. It is suggested that this geometrical difference is responsible for the lack of metal-metal interaction observed in the former, assuming the interaction is due to the overlap of axial metal orbitals.

ACKNOWLEDGEMENT

I greatly appreciate the advice and encouragement given by Professor D. Hall throughout this work.

I would also like to thank Professor M.J. Bennett for helpful advice.

Finally I gratefully acknowledge the financial assistance provided by the University of Alberta.

LIST OF FIGURES

Fig. Page

1. Representation of $F_{hk\ell}$ in the complex plane 13

For bipy(CO)$_3$BrWGeBr$_3$

2. Atomic labelling scheme 29
3. Thermal ellipsoids for the atoms - W, Ge, Br(1), Br(2), Br(3), Br(4). 32
4. Molecular packing - projection onto the [b][c] plane. 39
5. Molecular packing - projection onto the [a][c] plane. 40
6. Stereoscopic diagram of the molecular packing. 41
7. Capped trigonal prism arrangement of the Co-ordination atoms. 42
8. Approximation of (a) bipy(CO)$_3$BrWGeBr$_3$ and (b) bipy(CO)$_3$CℓMoSnCH$_3$Cℓ_2 to the tetragonal base-trigonal base geometry 43

For [Pt(etNH$_2$)$_4$][PtCℓ_4]

9. Atomic labelling scheme. 66
10. Ionic packing in the plane perpendicular to the [c] axis. 71
11. Ionic packing - projection onto the [a][c] plane. 72

LIST OF TABLES

Table Page

1. Heptaco-ordinate geometries 5

For bipy$(CO)_3BrWGeBr_3$

2. Structure amplitudes 28
3. Atomic co-ordinates and isotropic temperature factors. 30
4. Anisotropic temperature factors for the atoms - W, Ge, Br(1), Br(2), Br(3), Br(4). 31
5. Intramolecular bonding distances 33
6. Intramolecular non-bonding distances. 34
7. Selected intermolecular contacts less than 4.0 Å. 35
8. Bond angles 36

For $[Pt(etNH_2)_4][PtCl_4]$

9. Unit cell dimensions. 64
10. Structure factors 65
11. Atomic co-ordinates and isotropic temperature factors. 67
12. Intraionic distances (a) bonding and (b) non-bonding. 68
13. Bond angles. 69
14. Selected interionic distances less than 4.0Å 70

THE CRYSTAL STRUCTURE OF 2,2'-BIPYRIDYL(TRIBROMOGERMANIUM)μ-BROMOTRICARBONYL TUNGSTEN, (BIPY(CO)$_3$BrWGeBr$_3$)

Introduction

Compounds in which an atom is bonded to seven or more atoms are, with few exceptions, confined to elements in the second and third transition series, lanthanides and actinides. The majority of these compounds may be considered covalent in nature and classified as having unidentate ligands, multidentate ligands or clusters of atoms in which individual atoms have high coordination numbers. Their formation is attributed partly to the size and charge of the metal ions involved as well as to the availablility of metal d orbitals for bonding.

In regard to the availability of orbitals it is observed[2] that metal ions of d° or low d^x configurations form more high co-ordination structures than do metal ions of high d^x configurations and this suggests that the greater number of vacant low energy d orbitals found in the former type is an important factor in their formation. For example[2] in simple metal carbonyls or substituted metal carbonyls where the formation of a complex is dependent on utilizing all nine orbitals, large co-ordination numbers (in this case 8) are favored with metal ions of low d^x configurations such as Mo^V, W^{IV}, Re^{VI}. In addition, ions such as these in high oxidation states are able to acquire neutrality more readily by the

attachment of a large number of ligands. More high co-ordination compounds are found in the early transition series than in groups IIIb and IVb which follow, and this is also attributed[2] to energy differences between available orbitals (in this case s, p, and d). This trend cannot be completely dissociated, however, from the decrease in metal ion radii which occurs in a periodic series from configuration d^0 to d^{10}.[1]

While the possibility of high co-ordination for a particular species may be predicted with some degree of certainty there is no way as yet to successfully treat the bonding and hence predict geometries.[1] Some attempts have been made using valence bond approximations to assess bond overlap from purely symmetry arguments but their success is limited to a few examples only, one of which is the arrangement of ligands in octaco-ordination.[1] Only seven orbitals of the correct symmetry can be generated for the cubic arrangements unless f orbitals are used and this is consistent with the fact that the arrangement of ligands found in discrete molecular species is dodecahedral or antiprismatic rather than cubic. Most ground state geometries, including those for octaco-ordination mentioned above, are rationalized by applying the non-bonding repulsion

theory[3] which is based on the assumption that lone-pairs and σ bonding pairs of electrons arrange themselves as far apart as possible around any atom. This rather simple approach is found to be inadequate in the case of heptaco-ordination which includes three 'ideal' geometries, namely C_{3v}, C_{2v}, C_{5h}. Theoretical calculations[4] based on repulsive forces between identical ligands showed that the energy differences between the three are in fact only small fractions of the total energy and thus indicate that ground state configuration depends on something other than repulsive forces between ligands. It has been suggested,[1] that since the energy differences between isomers are smaller or comparable to packing forces in the solid state and solvation and association energies in the liquid state, no one ideal arrangement will exist for all three physical states, i.e. such forces may stabilize a geometry which is not the ground state geometry found in the unperturbed gaseous state.

While the similarity in energy of the 'ideal' heptaco-ordinate geometries has been demonstrated for identical ligands, it is conceivable that for certain mixtures of ligands one particular geometry will be of lower energy. For example pentagonal bipyramid (D_{5h}) for MX_5Y_2, capped trigonal prism (C_{2v}) or capped octahedron (C_{3v}) for MX_6Y and the tetragonal base-trigonal

base geometry (C_s) for MX_4Y_3. (Descriptions given in Table I). It seems reasonable to suppose that compounds containing less homogeneous mixtures of ligands will have geometries describable as distorted models of one or more of those mentioned above. The crystalline structure of one such compound is the subject of the first part of this thesis: bipy$(CO)_3BrWGeBr_3$ (type MA_2B_3CD) contains four chemically different ligands, including a bidentate ligand which is the only constraint placed on the molecular geometry.

2,2'-Bipyridyl(tri bromogermanium) μ-bromotricarbonyl tungsten, (bipy$(CO)_3BrWGeBr_3$) belongs to a series of compounds of the general formula bipy$(CO)_3$ MM"RX_2, where M ≡ W, Mo; M" ≡ Sn, Ge; X ≡ I^-, Br^-, Cl^-; R ≡ X or alkyl, in which tungsten and molybdenum are heptaco-ordinate.

A detailed study and comparison of the infrared spectra of these compounds in dichloromethane carried out by Kummer and Graham[5] led to several interesting observations. The carbonyl stretching region showed two distinct sets of three bands and the relative intensities of these sets, labelled I and II varied with the substituents; bands of set I became more intense in going from $Cl^- \rightarrow I^-$, Mo → W, Sn → Ge, $RSnX_3 \rightarrow SnX_4$ while those of set two became weaker. For example, bipy$(CO)_3IWGeI_3$ shows three bands designated as set I while bipy$(CO)_3ClMoSnCH_3Cl_2$

TABLE 1

HEPTACO-ORDINATE GEOMETRIES

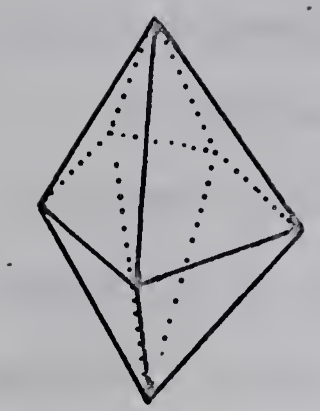

Pentagonal Bipyramid - D_{5h} symmetry

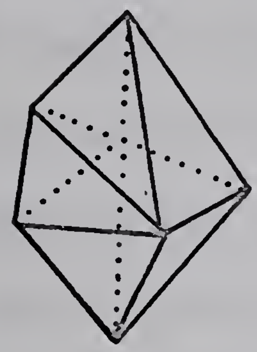

Capped Octahedron - C_{3v} symmetry. The seventh atom lies above the centre of one face of an octahedron which is distorted mainly by the spreading apart of the three atoms defining the face.

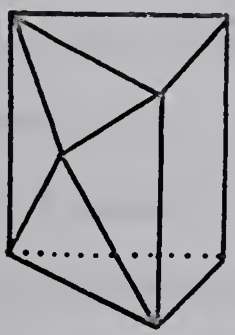

Capped Trigonal Prism - C_{2v} symmetry. The seventh atom sits above the centre of one of the rectangular faces of a trigonal prism.

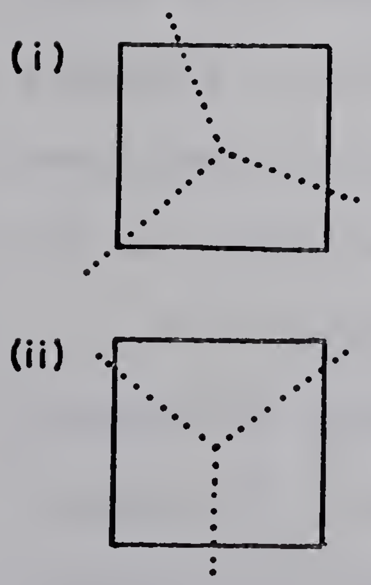

Tetragonal Base - Trigonal Base - C_s symmetry. A 4:3 distribution of ligands with an idealised 4 fold axis coincident with an idealised 3 fold axis. The two orientations (i and ii) are related by a 45° rotation of the four symmetry related ligands with respect to the other three ligands.

shows bands belonging to set II only. Compounds intermediate in this series however showed four or five distinct bands.

An explanation for this apparent anomaly was given by Kummer and Graham who suggested that the sets of bands I, II, resulted from two geometrical isomers. However, such a proposal remained pure conjecture without knowledge of the co-ordination geometry of the molecules. It seemed that the three dimensional crystal structure analyses of several of these compounds would be useful in elucidating the nature of the proposed isomers which almost certainly exist in solution.

Initial work on this series of compounds was done in this laboratory by Dr. M. Elder who determined the three dimensional crystal structure of bipy$(CO)_3C\ell MoSnCH_3C\ell_2$,[6] pure "isomer II". This shows it to contain an unexpected 5-co-ordinated tin and a 7-co-ordinated molybdenum atom which are bridged by a chlorine atom. The co-ordination geometry of the molybdenum atom is most accurately described in terms of a capped octahedral arrangement, the tin atom being at the centre of the capped face.

As a comparison with the above compound and for the purpose of establishing the co-ordination geometry of "isomer I", the three dimensional crystal structure analysis of bipy$(CO)_3BrWGeBr_3$ was undertaken. It should

be mentioned that bipy$(CO)_3BrWGeBr_3$ exists as a mixture of isomers in solution exhibiting four distinct bands rather than three in its infrared spectrum. The two compounds bipy$(CO)_3IMGeI_3$; M ≡ Mo, W, described as pure "isomer I", were found by Dr. M. Elder on preliminary investigation to be unsuitable for single crystal diffraction work.

Experimental

$Bipy(CO)_3BrWGeBr_3$ was prepared using a method of halogen exchange outlined by Kummer and Graham.[5] Crystals were supplied by Dr. Kummer for this structure determination.

On examining these crystals optically two distinct crystalline species were evident which could be distinguished readily by the their colour and quality. Those coloured red were prismatic in shape with several well developed faces, while those coloured dark green were of a similar form but had poorly developed faces. Crystals of both types were examined by photography. The green crystals gave very diffuse spots and trace powder patterns indicating either some disorder in the molecules or more probably that the crystals were not single but microcrystalline and this was supported by their tendency to break into tiny crystallites on touching. The crystal diffraction symmetry (monoclinic) and cell dimensions ([a] = 7.6 Å, [b] = 13.2 Å, [c] = 6.9 Å, β = 103°) were obtained from precession photographs of one of the better crystals. Because of the quality and limited number of reflections these parameters are not very reliable and further the space group could not be determined. Further work on the green compound at this stage seemed pointless as the superior quality of the red crystals made them the obvious choice for a 3-dimensional structure analysis; all

following discussions are concerned with the "red" compound.

Weissenberg photographs of several crystals were collected for layers $0k\ell$, $1k\ell$, $2k\ell$, $3k\ell$, $h0\ell$. These showed 2/m diffraction symmetry and systematic absences, $h0\ell$ for ℓ odd and $0k0$ for k odd, consistent with the monoclinic space group $P2_1/c$. The unit cell parameters were determined from $h0\ell$ and $hk0$ precession photographs using Cu Kα radiation (λ = 1.5418 Å) to give

[a] = 8.62 ± 0.01 Å
[b] = 16.50 ± 0.02 Å
[c] = 13.58 ± 0.01 Å
[β] = 90.3 ± 0.2°

The observed density, measured by flotation in a solution of dibromomethane and diiodomethane, was 2.73 compared to 2.81 for that calculated with $z = 4$, $V = 1931.4$ Å^3 and M.W. = 816.4. With 4 molecules per unit cell each must occupy one of the four general positions belonging to space group $P2_1/c$, namely: (x, y, z); $(\bar{x}, \bar{y}, \bar{z})$; $(x, \frac{1}{2} - y, \frac{1}{2} + z)$; $(\bar{x}, \frac{1}{2} + y, \frac{1}{2} - z)$.

Intensity data were collected on a Pailred Linear diffractometer with the crystal (dimensions (0.258 x 0.129 x 0.129) mm along [a], [b], [c] respectively) mounted about the [a] axis. Crystal monochromatised

Mo Kα radiation (λ = 0.7107 Å) was used in preference to Cu Kα radiation to minimize absorption effects as μ_{Mo} = 178 cm^{-1}, μ_{Cu} = 242 cm^{-1}. Using a counter aperture of 2°, each reflection was scanned at the rate of 1°/min for a period (increasing with h) of 60 to 180 secs and the background was counted each side of the peak for a total of 40 secs. Of the 2900 independent reflections measured 1800 were rejected during initial processing of the data as they failed to qualify in the following tests:-

(i) $I > 0$

(ii) $\frac{\sigma I}{I} \leq 0.35$

where I is the total scan less the scaled background, $T - t(b_1 + b_2)$ and σI is $(T + t^2b)^{\frac{1}{2}}$. These 1100 observed reflections had a maximum sinθ value of 0.43 giving a resolution of approximately 0.7 Å in the three directions, [a], [b], [c]. Six reflections 040, 080, 180, 350, 230, 200 were checked before each layer was collected and the insignificant fluctuations in their intensities indicated there was no crystal decomposition. Corrections for Lorentz and Polarization effects were made and structure amplitudes derived.

Structure Determination

Atomic Scattering Factor

The scattering factor, f_o, relates the scattering power of an atom to that of an equivalent number of electrons positioned at the atomic nucleus. Because beams scattered by electrons are out of phase to a greater extent at high values of $\sin\theta$, this function decreases with increase of $\sin\theta/\lambda$.

Scattering factor curves are calculated assuming electrons are distributed in a stationary atom while in fact atoms in crystal are continuously vibrating. These vibrations, which reduce the scattering efficiency of an atom, may be accounted for by applying a term of the form $\exp-(B\sin^2\theta/\lambda^2)$ to the scattering factor curve, f_o; where B (isotropic temperature factor) $= 8\pi^2\bar{u}^2$ and $\bar{u}^2$ is the mean-square amplitude of atomic vibration. Thus the proper scattering factor for a real atom is given by $f = f_o\exp-(B\sin^2\theta/\lambda^2)$.

The above equation still assumes spherical vibration but since real atoms do not vibrate spherically a more appropriate temperature factor, known as the anisotropic temperature factor which consists of six parameters defining an ellipse, may be used.

Anomalous Dispersion

X-radiation being electromagnetic radiation has associated with it an alternating electromagnetic field. An electron forced into oscillation by this field in turn becomes a source of scattered electromagnetic radiation. The waves scattered in this manner will be in or out of phase depending on the binding energy of an electron as compared to the quantum energy of radiation. In particular when the frequency of the primary radiation is just above that corresponding to an absorption edge of the scattering atom, the contribution to the scattering factor of the K electrons (most tightly bound electrons) will be out of phase with the other electrons i.e. the wave scattered by the atom has had an anomalous phase shift. Thus a real and imaginary correction is made to the normal scattering factor: $f = f_o + \Delta f' + i\Delta f''$. In non-centrosymmetric structures in which some of the atoms exhibit anomalous dispersion there is a breakdown of Friedels Law and $|F_{hk\ell}|^2 \neq |F_{\overline{hk\ell}}|^2$.

The Structure Factor

A wave may be described in terms of a point moving on a circle at a constant angular velocity i.e. a rotating vector. Since waves scattered by an atom have the same velocity but different amplitudes and phases

they may be represented as static vectors in the complex plane. The vector representation for a wave of amplitude f_1 and phase angle ϕ_1 (with respect to the wave scattered by hypothetical electrons at the cell origin) is $f_1 \exp i\phi_1$. Thus the structure factor, $F_{hk\ell}$, defined as the resultant sum of j waves scattered by j atoms in the direction of the scattering vector to the hkℓ is given by

$$F_{hk\ell} = \sum_j f_j \exp i\phi_j \quad \text{(see Fig. 1 below).}$$

Figure (1)

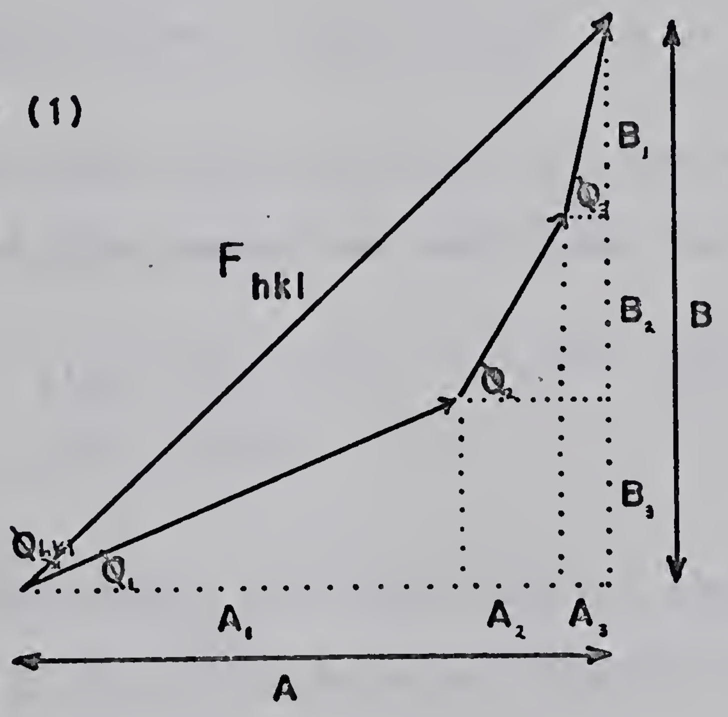

The phase angle, ϕ_j, may be expressed in terms of hkℓ and the fractional co-ordinates, (x_j, y_j, z_j), of the atoms in the cell: $\phi_j = 2\pi(hx_j + ky_j + \ell z_j)$ so that

$$F_{hk\ell} = \sum_j f_j \exp i2\pi(hx_j + ky_j + \ell z_j) \qquad ..(1)$$

Equation (1) may be resolved into real and imaginary components such that

$$F_{hk\ell} = \sum_j f_j \cos 2\pi(hx_j + ky_j + \ell z_j) + i\sum_j f_j \sin 2\pi(hx_j + ky_j + \ell z_j)$$

which may be abbreviated to $F_{hk\ell} = A + iB$ where

$$A = \Sigma f_j \cos 2\pi(hx_j + ky_j + \ell z_j)$$

and ..(2)

$$B = \Sigma f_j \sin 2\pi(hx_j + ky_j + \ell z_j)$$

Fig. (1) shows that the magnitude of the structure factor, $|F_{hk\ell}|$, called the structure amplitude is:

$$\begin{aligned}|F_{hk\ell}| &= [(A_1 + A_2 + A_3 + \ldots)^2 + (B_1 + B_2 + B_3 + ..)^2]^{\frac{1}{2}} \\ &= [A^2 + B^2]^{\frac{1}{2}}\end{aligned}$$

This may be expressed as a function of the co-ordinates of the atoms in the cell by substituting in equation (2):

$$|F_{hk\ell}| = [(\sum_j f_j \cos 2\pi(hx_j + ky_j + \ell z_j))^2 + (\sum_j f_j \sin 2\pi(hx_j + ky_j + \ell z_j))^2]^{\frac{1}{2}} \quad ..(3)$$

The above equation is used in computations to evaluate $|F_{hk\ell}|$.

An important simplification of equation (3) occurs for a centrosymmetric structure, in which an atom having co-ordinates, (xyz), is accompanied by an atom at $(\bar{x}, \bar{y}, \bar{z})$. Substitution of these co-ordinates into equation (2) gives:

$$A = 2\sum_j f_j \cos 2\pi(hx_j + ky_j + \ell z_j)$$

where summation is over half the atoms in the unit cell and B = 0. Thus the phase angle, $\phi_{hk\ell} = \tan^{-1} \frac{B}{A}$ (Fig. 1), can have only one of two values 0 or π and this means that the evaluation of the structure factor, $F_{hk\ell}$, reduces to the assignment of + or - sign to the structure amplitude $|F_{hk\ell}|$.

Fourier Synthesis

A periodic function may be represented by a summation of cosine and sine terms known as a Fourier series and since a crystal is periodic, its electron density can be represented by such a series. The following equation gives the 3-dimensional periodic electron density at a point (x, y, z) in the unit cell, where m, n, o are integers between - and + infinity.

$$\rho_{xyz} = \sum_m \sum_{n=-\infty}^{+\infty} \sum_o C_{mno} \exp(2\pi i(mx + ny + oz))$$

On substitution of ρ_{xyz} into the structure factor expression:

$$F_{hk\ell} = \int_V \rho_{xyz} \exp(2\pi i(hx + ky + \ell z))dV \text{ and}$$

simplifying, it can be shown that the Fourier coefficients $C_{mno} = \frac{1}{V} \cdot F_{hk\ell}$ and m, n, o are identical to the Miller indices, $\overline{hk\ell}$. Thus the 3-dimensional Fourier synthesis of the electron density can be written as:

$$\rho_{xyz} = \frac{1}{V} \sum_h^{+\infty} \sum_k \sum_\ell {}_{-\infty} F_{hk\ell} \exp(-2\pi i(hx + ky + \ell z)) \quad ..(4)$$

An alternative expression for a 3-dimensional Fourier synthesis can be obtained by substituting $F_{hk\ell}$ for $|F_{hk\ell}| \exp i2\pi\, \alpha_{hk\ell}$ in equation (4) and expanding in terms of cosines and sines. If Friedels Law is assumed the sine terms will cancel for pairs of $F_{hk\ell}$ and $F_{\overline{hk\ell}}$ and the following simplified expression will be obtained.

$$\rho_{xyz} = \frac{1}{V} \sum_h \sum_k \sum_\ell |F_{hk\ell}| \cos 2\pi(hx + ky + \ell z - \alpha_{hk\ell})$$

This expresses the electron density in terms of the structure amplitudes, which are determined experimetally, and the phase angle. Thus the Fourier synthesis is limited to uses other than direct structure solution as the phase angle cannot be measured experimentally.

If one or two atoms are located by methods requiring no prior knowledge of phases such as the Patterson synthesis

(described in next section) the phase of their contributions to the structure factor can be calculated. By accepting these phase angles, the Fourier synthesis may be used to complete the structure determination. This method of solution is particularly effective when the structure contains one or two heavy atoms in the presence of light ones so that the contribution from these heavy atoms dominates that of the light atoms and consequently the heavy atom phase is a close approximation to the resultant phase.

In practice Fourier syntheses are not summed from + to - infinity but within certain limits of $hk\ell$, largely dependent on the radiation used. This gives rise to series termination errors which appear as diffraction ripples around atomic positions on the Fourier map. As a result in heavy atom structures particularly, light atom peaks close to the heavy atoms are often obscured. This problem may be overcome by using the difference between observed and calculated structure amplitudes as coefficients in the electron density expression. The series termination errors in both Fourier summations, i.e. one with coefficient F_o, and one with coefficient F_c, are almost identical and hence cancel each other out to give a difference synthesis essentially free from errors.

Patterson Synthesis

The Patterson function defined as:

$$P_{uvw} = V\int_{x}\int_{y}\int_{z} \rho_{(x,\ y,\ z)} \cdot \rho_{(x\ +\ u,\ y\ +\ v,\ z\ +\ w)}\, dx,dy,dz \quad ..(5)$$

is a summation of the products of electron density of all points separated by the vector, u, v, w. If the electron density terms are expanded and the resulting function simplified assuming normal scattering conditions the following more calculable form of the Patterson expression is obtained

$$P_{uvw} = \frac{1}{V} \sum_{h} \sum_{k} \sum_{\ell} |F_{hk\ell}|^2 \cos 2\pi (hu + kv + \ell w)$$

Unlike the Fourier (electron density) synthesis this can be evaluated using the experimentally observed, structure amplitudes. While the Fourier synthesis gives the distributions of atoms in a cell, the Patterson synthesis contains peaks corresponding to all the atomic vectors. It is evident from equation (5) that P_{uvw} will have large values when $\rho_{x,y,z}$ and $\rho_{x+u,\ y+v,\ z+w}$ are both large, i.e. when the vector, u, v, w corresponds to an interatomic vector between two atoms. Since the magnitude of a Patterson peak is approximately proportional to the product of the atomic numbers of the two atoms involved, the vector peaks

between heavy atoms will be much larger than surrounding peaks (heavy-light, light-light vectors), thus affording ready identification. Although positions of all atoms in a structure can be determined from a Patterson map, in practise the approximate coordinates of the heavy atoms only are derived and the structure is completed by the method of Fourier synthesis as previously described.

As the Patterson function is a product of electron densities its peaks will appear diffuse. This condition may be improved by a process known as sharpening which effectively concentrates the electrons in an atom at the nucleus, i.e. the atoms become ideally point atoms. One property of a point atom is that its scattering efficiency is invariant (equal to z, atomic number) with $\sin\theta/\lambda$. While $f = z$ for point atoms, $f = f_o \exp(-\sin^2\theta/\lambda^2)$ for real atoms which possess thermal motion. Hence F for point atoms may be expressed in terms of F for real atoms by:

$$F_{point} = z/f_o \exp(-\sin^2\theta/\lambda^2) . F_{real}$$

assuming the cell only contains one kind of atom. In practice, because most structures contain several kinds of atoms, some average value of z/f_o must be used such that

$$F_{point} = \frac{\sum_{i=1}^{N} z_i}{\exp(-B\sin^2\theta/\lambda^2) . \sum_{i=1}^{N} f_{oi}} . F_{real}$$

The $|F_{points}|$ so obtained can be squared and used as coefficients for a sharpened Patterson function.

If a unit cell contains N atoms, the Patterson function will give N^2 peaks in vector space. N of these will be vectors of zero length from each atom to itself and will be concentrated in a very large peak at the origin. The origin peak, which is superfluous, may be removed from a sharpened Patterson map by subtracting the quantity $\sum_{i=1}^{N} z_i^2$ from each $|F_{point}|^2$ coefficient. The remaining N^2-N peaks will be distributed throughout the cell and will include vector peaks from symmetry related atoms. Such peaks, known as Harker peaks, facilitate interpretation of the Patterson map as they may have one or more of their co-ordinates fixed, depending on the symmetry operation relating the atoms. The different types of Harker peaks found are:

(i) Those which occur between centrosymmetrically related atoms i.e. (2x, 2y, 2z) and have no fixed co-ordinates.

(ii) Those between atoms related by a rotation or screw axis. These vectors have one fixed co-ordinate and are found on the Harker section.

(iii) Those between atoms related by a mirror or

glide plane. Such vectors have two fixed co-ordinates and are found on the Harker line.

For example in space group $P2_1/c$ the four general atomic positions with their corresponding symmetry element referred to atom at (x, y, z) are:

x, y, z	1
$\bar{x}, \bar{y}, \bar{z}$	$\bar{1}$
$\bar{x}, \frac{1}{2} + y, \frac{1}{2} - z$	2_1
$x, \frac{1}{2} - y, \frac{1}{2} + z$	c

The three unique vectors derived from these are:

$$(2x, 2y, 2z);\ (2x, \tfrac{1}{2}, \tfrac{1}{2} + 2z);\ (0, \tfrac{1}{2} + 2y, \tfrac{1}{2}).$$

with multiplicities of 1, 2, 2 respectively.

Structure Solution and Refinement

The space group $P2_1/c$ was confirmed on cursory examination of the sharpened three dimensional Patterson synthesis (p. 18) by the presence of a large number of peaks on the Harker line, $(0, \frac{1}{2} + 2y, \frac{1}{2})$, and the Harker section, $(2x, \frac{1}{2}, \frac{1}{2} + 2z)$. By analysing the largest vector peaks on these sections the positional co-ordinates of the tungsten atom were readily derived. This assignment

of vectors on the basis of peak height is justifiable in the case of tungsten as it has twice as many electrons as the next heaviest atom, bromine. The choice was further confirmed by the (2x, 2y, 2z) vector (i.e. the vector between centrosymmetrically related tungsten atoms) which was the largest peak in general space. In order to locate as many of the heavy atoms as possible several large vectors within a 4 Å radius of the origin were chosen as cross vectors between the tungsten and these atoms. The cross vectors may be represented as $(x_w - x_p)$, $(y_w - y_p)$, $(z_w - z_p)$ where subscripts w and p denote tungsten and other heavy atoms respectively. Use was made of the tungsten co-ordinates, (x_w, y_w, z_w), previously found for determining other atomic positions, (x_p, y_p, z_p), and Harker vectors derived from these new co-ordinates were than checked. In this way the heavy atoms bonded to the tungsten (i.e. a germanium and bromine atom) and two of the three bromine atoms bonded to the germanium atom were located.

A structure factor calculation (p 12) based on these five atoms with $B_{iso} = 3.0$ Å^2 for all atoms gave a discrepency index $R = 0.363 = \Sigma||F_o| - |F_c||/\Sigma |F_o|$ where F_o and F_c are the observed and calculated structure factors respectively and an F_o Fourier synthesis done at the same time revealed the position of the third bromine

atom bonded to the germanium. After one refinement cycle, using block diagonal least squares and varying the scale factor, positional parameters and isotropic temperature factors of the six heavy atoms, the discrepency index, R, was 0.276. All the light atoms were subsequently located from an F_o Fourier synthesis phased with the heavy atoms. Refinement was continued for several cycles in the same manner as mentioned above but with all atoms included, reducing the R index to 0.158. Three further cycles of refinement using full matrix least squares, only reduced the R index to 0.153 and from the small shifts in most parameters it appeared that the limit in refinement of the isotropic model had been reached. This observation together with the presence of large peaks either side of the heavy atom positions on the difference Fourier map (p. 15) prompted the conversion from isotropic to anisotropic temperature factors. Anisotropic temperature factors of the form

$$\exp-(\beta_{11}h^2 + \beta_{22}k^2 + \beta_{33}\ell^2 + 2\beta_{12}hk + 2\beta_{23}k\ell + 2\beta_{31}h\ell)$$

were calculated for all atoms but those for the light atoms proved to be physically meaningless. Several refinement cycles using full matrix least squares in which the scale factor, all positional parameters, anisotropic temperature factors for the heavy atoms and isotropic temperature factors for the light atoms were varied, resulted in a

convergence with $R = 0.102$ and $R_w(=(\Sigma w[|F_o| - |F_c|]^2/\Sigma w|F_o|^2)^{\frac{1}{2}}) = 0.112$ using unit weights ($w = 1$). A final difference Fourier map showed residual density from -2 to +2 electrons around some heavy atom positions but all other residual electron density varied in height from -1 to +1 electrons with the exception of one peak of 2 electrons situated between the tungsten atom and C(13) (the height of a carbon atom on the same scale is 6 electrons). Several large low $\sin\theta$ reflections apparently suffering from extinction were removed, and absorption corrections were made in the hope of reducing errors in atomic co-ordinates and hence bond lengths. This was accomplished using a programme, written by C.T. Prewitt which evaluates the transmission factor, T, for a particular $hk\ell$ reflection from the equation: $T = \frac{1}{V}\int^{V} e^{-\mu p} dV$ where μ = linear absorption coefficient, p = total pathlength of the primary and diffracted X-ray beams inside the crystal for the volume element dV. At this stage, diffractometer weights were used in place of the conventional weighting scheme mentioned earlier; the new weights are calculated using $\sigma = (T + t^2B + (KI)^2)^{\frac{1}{2}}$ where $I \equiv$ intensity, $t \equiv$ total count time/total background time, $B \equiv$ total background count.[17] The standard deviation of an

observation of unit weight $((\Sigma_w\Delta^2/n - m)^{\frac{1}{2}}$, where n is the number of observations, m is the number of parameters varied) was 2.25 and this value was obtained with K = 0.06. Further refinement only reduced the discrepency index slightly to give R = 0.100 and R_w = 0.108.

The atomic scattering factors for all above calculations were from the International Tables[7] with real dispersion corrections, Δf', (p.12) applied to the tungsten and bromine curves. In the final cycle, however, corrections for the imaginary part of the anomalous dispersion, Δf", were included since it has been established[8] that, while neglect of Δf" will not affect co-ordinates of atoms in centrosymmetric structures, errors may arise in vibrational parameters if this term is neglected.

Results

Table 2 gives the observed, F_o, and calculated, F_c, structure amplitudes on the absolute scale (in electrons) x 10. A complete molecule is shown in Figure 2 with the atomic labelling scheme used. The final atomic co-ordinates for all atoms and isotropic temperature factors for the light atoms are listed in Table 3. In this table and those following, standard deviations in the least significant figures are given in parentheses. The anisotropic thermal vibrations of the six heavy atoms (W, Ge, Br(1), Br(2), Br(3), Br(4)) are given in Table 4 as U_{ij}s which are in terms of mean-square amplitudes of vibration in $\mathring{A}^2$ referred to the unit cell axes. The general temperature factor expression involving these U_{ij}'s is

$$\exp[-2\pi^2(U_{11}h^2a^{*2} + U_{22}k^2b^{*2} + U_{33}\ell^2c^{*2} + 2U_{12}hka^*b^*\cos\gamma^* + 2U_{13}h\ell a^*c^*\cos\beta^* + 2U_{23}k\ell b^*c^*\cos\alpha^*)].$$

These atomic vibrations are depicted in Figure 3 which shows the relative magnitude of vibrations along the major axes of the thermal ellipsoids. All appear to be physically reasonable with the largest vibration perpendicular to the relevant bond direction. Interatomic distances and bond angles are listed in Tables 5, 6,7, and

8 and the packing of the molecules in the [b][c] and [a][c] planes is depicted in Figures 4 and 5 respectively. Figure 6 gives a three dimensional picture of the molecular packing when viewed with the appropriate lenses (in back cover of this thesis).

TABLE 2

STRUCTURE AMPLITUDES ON THE ABSOLUTE SCALE x 10

FIGURE 2

A COMPLETE MOLECULE WITH THE ATOMIC LABELLING SCHEME

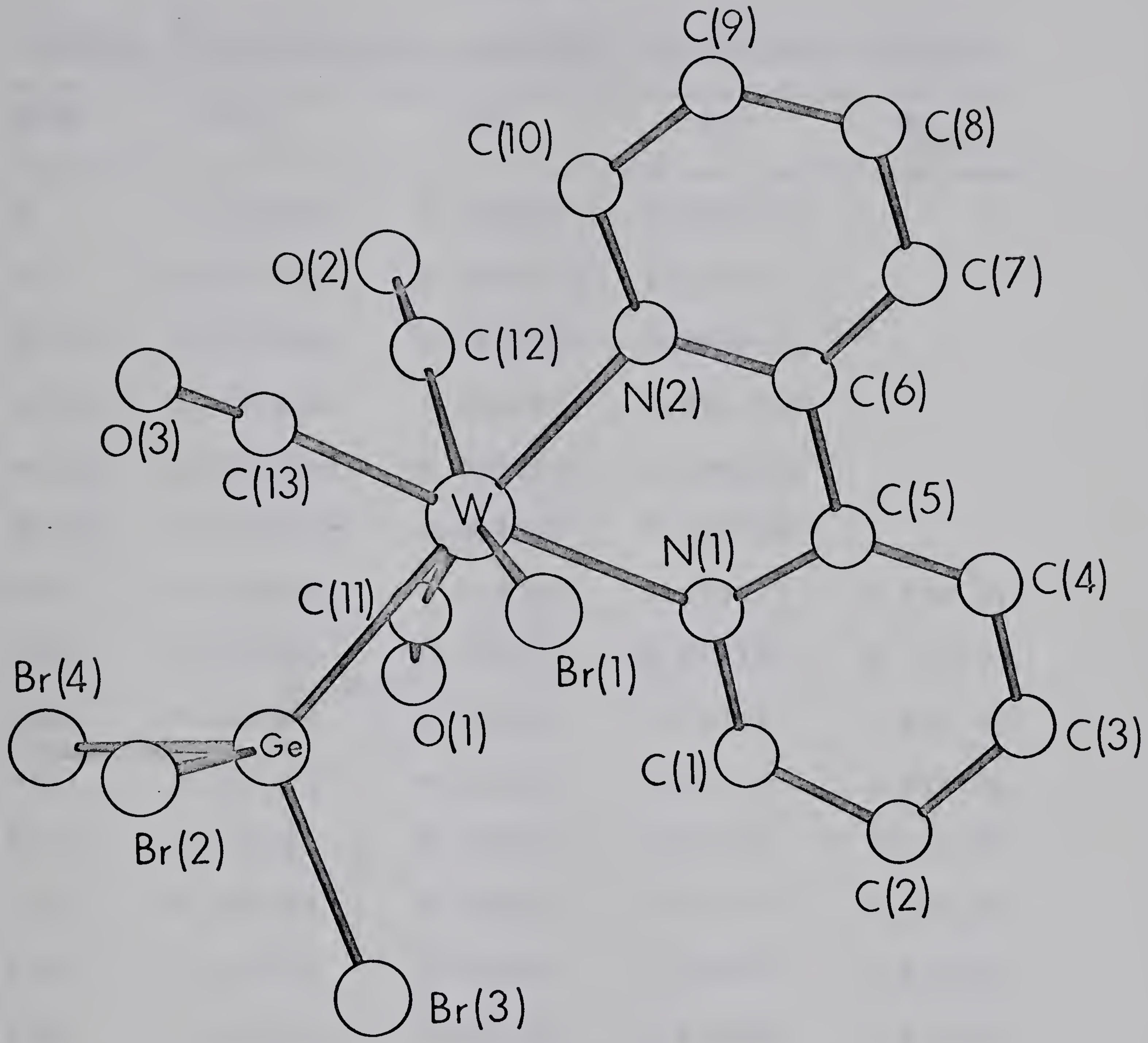
C(9)
C(10)
C(8)
O(2)
C(7)
C(12)
O(3)
N(2)
C(6)
C(13)
W
C(5)
N(1)
C(4)
C(11)
Br(4)
Br(1)
O(1)
Ge
C(1)
C(3)
Br(2)
C(2)
Br(3)

TABLE 3

ATOMIC COORDINATES AND ISOTROPIC TEMPERATURE FACTORS

Atom	x/a	y/b	z/c	B_{iso}
W	0.3249(2)	0.1983(1)	0.3478(2)	
Ge	0.4270(6)	0.0816(4)	0.2360(4)	
Br(1)	0.0683(6)	0.1476(4)	0.2669(5)	
Br(2)	0.3324(8)	0.0679(5)	0.0797(5)	
Br(3)	0.4013(9)	-0.0482(4)	0.2992(6)	
Br(4)	0.6893(7)	0.0848(5)	0.1979(6)	
O(1)	0.608(4)	0.119(2)	0.452(3)	5.4(0.9)
O(2)	0.564(5)	0.330(3)	0.411(3)	6.7(1.0)
O(3)	0.428(5)	0.272(3)	0.148(3)	7.2(1.1)
N(1)	0.206(5)	0.146(3)	0.477(3)	4.3(0.9)
N(2)	0.164(5)	0.290(3)	0.407(3)	4.3(0.9)
C(1)	0.240(6)	0.068(3)	0.515(4)	4.5(1.3)
C(2)	0.138(7)	0.029(4)	0.585(4)	5.1(1.3)
C(3)	0.013(6)	0.079(4)	0.625(4)	5.1(1.4)
C(4)	-0.014(6)	0.157(4)	0.590(4)	4.7(1.3)
C(5)	0.080(5)	0.184(3)	0.519(3)	2.1(0.9)
C(6)	0.061(4)	0.265(2)	0.479(3)	1.4(0.8)
C(7)	-0.058(6)	0.318(3)	0.510(4)	4.0(1.1)
C(8)	-0.078(6)	0.393(3)	0.463(4)	4.4(1.2)
C(9)	0.023(6)	0.417(3)	0.390(4)	4.1(1.2)
C(10)	0.148(7)	0.366(4)	0.356(4)	6.2(1.5)
C(11)	0.504(6)	0.152(3)	0.401(4)	4.7(1.3)
C(12)	0.469(6)	0.285(3)	0.389(4)	4.6(1.3)
C(13)	0.385(6)	0.249(4)	0.226(4)	4.7(1.3)

TABLE 4

ANISOTROPIC TEMPERATURE FACTORS

Atom	U_{11}	U_{22}	U_{33}	U_{12}	U_{13}	U_{23}	Equivalent B_{iso}
W	0.026(1)	0.043(1)	0.057(2)	0.000(1)	0.001(1)	0.003(2)	3.3
Ge	0.031(3)	0.053(4)	0.052(4)	-0.002(3)	0.002(3)	0.002(3)	3.6
Br(1)	0.035(3)	0.075(5)	0.080(5)	-0.009(3)	-0.003(3)	-0.010(4)	5.0
Br(2)	0.070(5)	0.102(6)	0.093(6)	-0.008(4)	-0.007(4)	-0.007(5)	7.0
Br(3)	0.096(5)	0.062(5)	0.109(6)	0.011(4)	0.034(5)	0.012(4)	7.0
Br(4)	0.048(4)	0.136(7)	0.104(6)	0.004(4)	0.014(4)	-0.001(5)	7.6

FIGURE 3

THERMAL ELLIPSOID DIAGRAM OF THE ATOMS -

W, Ge, Br(1), Br(2), Br(3), Br(4)

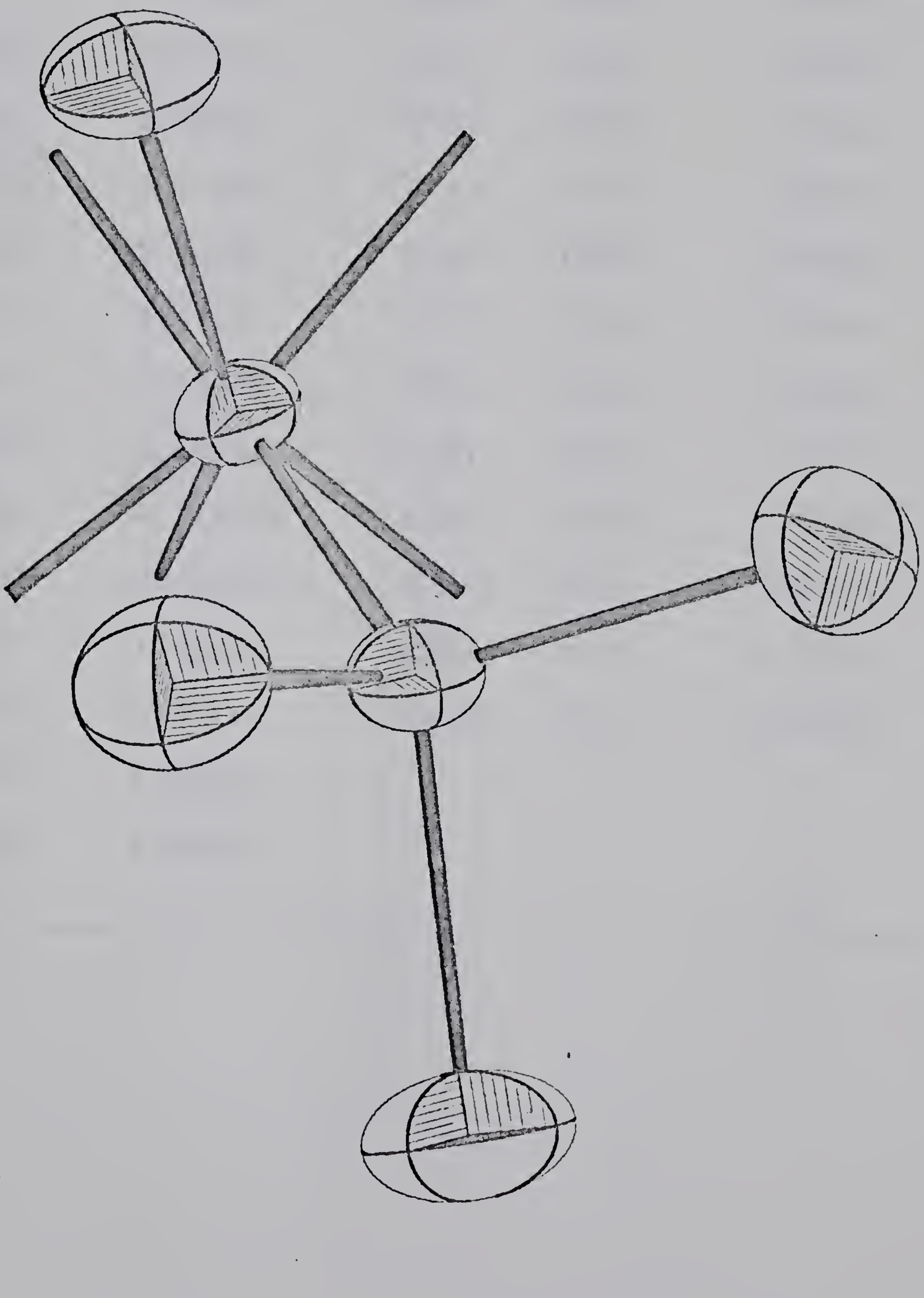

TABLE 5

INTRAMOLECULAR BONDING DISTANCES

Atom A	Atom B	Bond length in Å	Atom A	Atom B	Bond length in Å
W	Ge	2.608(6)	C(1)	C(2)	1.45(8)
W	Br(1)	2.603(6)	C(2)	C(3)	1.45(8)
W	C(11)	1.86(6)	C(3)	C(4)	1.39(8)
W	C(12)	1.97(6)	C(4)	C(5)	1.35(7)
W	C(13)	1.92(6)	C(5)	C(6)	1.44(6)
W	N(1)	2.21(4)	C(6)	C(7)	1.41(6)
W	N(2)	2.20(4)	C(7)	C(8)	1.41(8)
Ge	Br(2)	2.280(9)	C(8)	C(9)	1.38(8)
Ge	Br(3)	2.319(9)	C(9)	C(10)	1.45(8)
Ge	Br(4)	2.322(8)	C(11)	O(1)	1.26(7)
N(1)	C(1)	1.41(7)	C(12)	O(2)	1.14(7)
N(1)	C(5)	1.39(6)	C(13)	O(3)	1.19(7)
N(2)	C(6)	1.38(6)			
N(2)	C(10)	1.44(8)			

TABLE 6

INTRAMOLECULAR NON-BONDING DISTANCES

Atom A	Atom B	Distance in Å	Atom A	Atom B	Distance in Å
W	C(1)	3.21	Br(2)	Br(3)	3.59
W	C(5)	3.16	Br(2)	Br(4)	3.47
W	C(6)	3.09	Br(2)	C(13)	3.61
W	C(10)	3.16	Br(2)	O(3)	3.60
W	O(1)	3.10	Br(3)	Br(4)	3.59
W	O(2)	3.11	Br(3)	C(1)	3.78
W	O(3)	3.11	Br(3)	C(11)	3.68
Ge	Br(1)	3.31	Br(3)	O(1)	3.88
Ge	C(11)	2.60	Br(4)	C(11)	3.37
Ge	C(13)	2.78	Br(4)	C(13)	3.79
Ge	O(1)	3.37	Br(4)	O(1)	3.56
Ge	O(3)	3.37	Br(4)	O(3)	3.89
Br(1)	Br(2)	3.67	C(11)	C(12)	2.23
Br(1)	C(13)	3.25	C(11)	C(13)	3.03
Br(1)	N(1)	3.08	C(12)	C(13)	2.40
Br(1)	N(2)	3.13	C(11)	N(1)	2.77
			C(12)	N(2)	2.64

TABLE 7

SELECTED INTERMOLECULAR CONTACTS LESS THAN 4.0 Å

Atom A	Atom B	Distance in Å	Symmetry Transformation to be applied to Atom A
Br(1)	Br(4)	3.55	1+x, y, z
Br(2)	C(10)	3.60	x, ½-y, ½+z
Br(2)	O(2)	3.48	x, ½-y, ½+z
Br(2)	N(2)	3.62	x, ½-y, ½+z
Br(2)	C(8)	3.67	$\bar{x}$, ½+y, ½-z
Br(3)	O(1)	3.58	1-x, $\bar{y}$, 1-z
Br(3)	O(2)	3.51	1-x, ½+y, ½-z
Br(3)	O(3)	3.38	1-x, ½+y, ½-z

TABLE 8

BOND ANGLES IN DEGREES

Atom A	Atom B	Atom C	
Ge	W	Br(1)	78.8(2)
Ge	W	C(11)	69(2)
Ge	W	C(12)	119(2)
Ge	W	C(13)	74(2)
Ge	W	N(1)	109(1)
Ge	W	N(2)	159(1)
Br(1)	W	C(11)	137(2)
Br(1)	W	C(12)	152(2)
Br(1)	W	C(13)	91(2)
Br(1)	W	N(1)	79(1)
Br(1)	W	N(2)	81(1)
C(11)	W	C(12)	71(2)
C(11)	W	C(13)	106(3)
C(11)	W	N(1)	85(2)
C(11)	W	N(2)	132(2)
C(12)	W	C(13)	76(2)
C(12)	W	N(1)	111(2)
C(12)	W	N(2)	78(2)
C(13)	W	N(1)	168(2)
C(13)	W	N(2)	101(2)
N(1)	W	N(2)	72(2)

Table 8 cont'd

Atom A	Atom B	Atom C	
W	Ge	Br(1)	50.5(2)
W	Ge	Br(2)	119.7(3)
W	Ge	Br(3)	115.7(3)
W	Ge	Br(4)	116.4(3)
Br(2)	Ge	Br(3)	102.6(4)
Br(2)	Ge	Br(4)	98.0(3)
Br(3)	Ge	Br(4)	101.4(3)
W	C(11)	O(1)	168(5)
W	C(12)	O(2)	173(5)
W	C(13)	O(3)	173(5)
W	N(1)	C(1)	124(3)
W	N(1)	C(5)	121(3)
C(1)	N(1)	C(5)	115(4)
W	N(2)	C(10)	119(3)
W	N(2)	C(6)	117(3)
C(6)	N(2)	C(10)	123(4)
C(2)	C(1)	N(1)	121(5)
C(1)	C(2)	C(3)	117(5)
C(2)	C(3)	C(4)	121(5)
C(3)	C(4)	C(5)	117(5)
C(4)	C(5)	C(6)	121(4)

Table 8 cont'd.

Atom A	Atom B	Atom C	
C(4)	C(5)	N(1)	128(4)
C(6)	C(5)	N(1)	111(4)
C(5)	C(6)	C(7)	123(4)
C(5)	C(6)	N(2)	118(4)
C(7)	C(6)	N(2)	120(4)
C(6)	C(7)	C(8)	120(4)
C(7)	C(8)	C(9)	120(5)
C(8)	C(9)	C(10)	122(5)
C(9)	C(10)	N(2)	115(5)

FIGURE 4

MOLECULAR PACKING DIAGRAM PROJECTION ONTO THE [b][c] PLANE

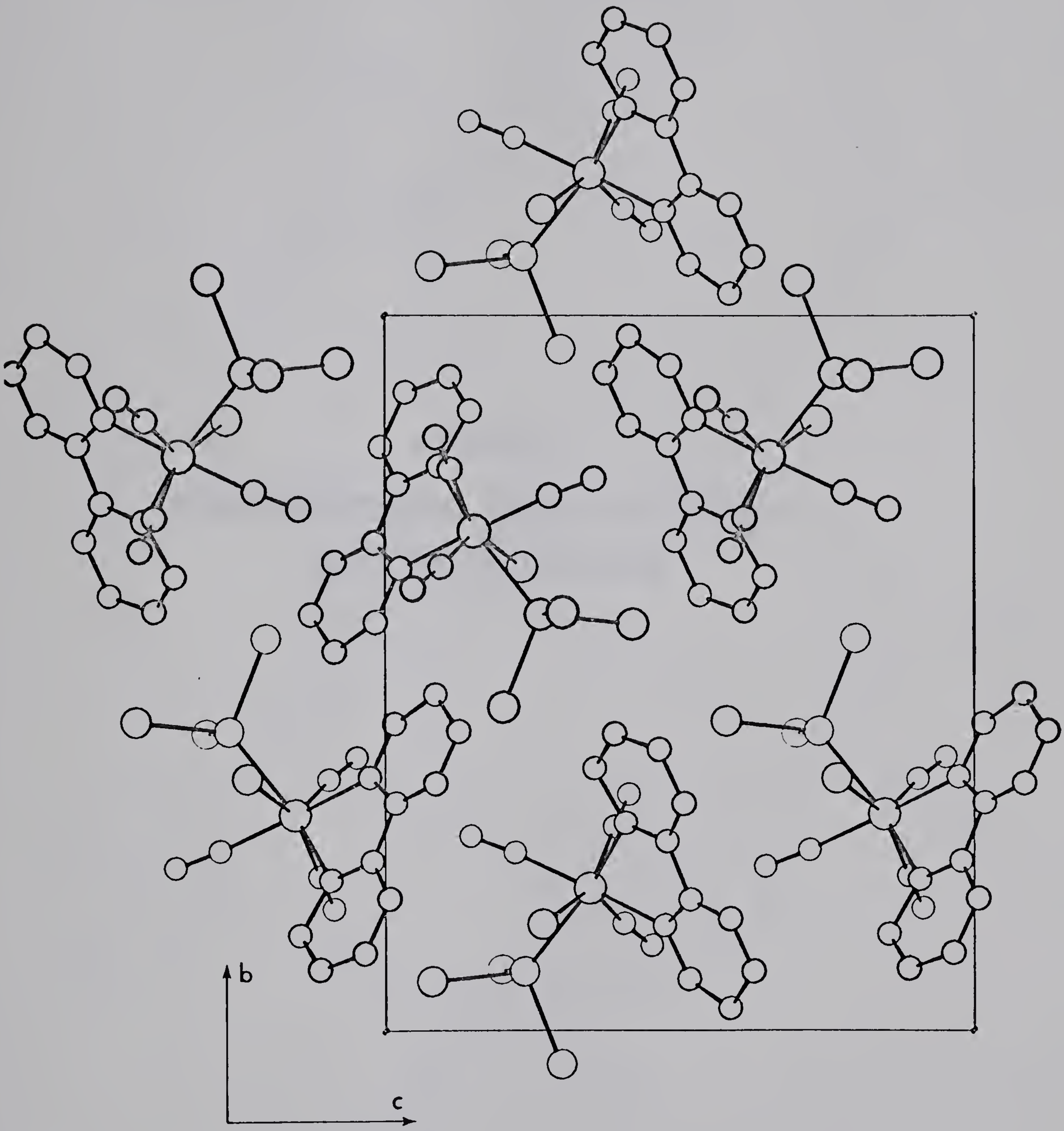
b
c

FIGURE 5

MOLECULAR PACKING DIAGRAM PROJECTION
ONTO THE [a][c] PLANE

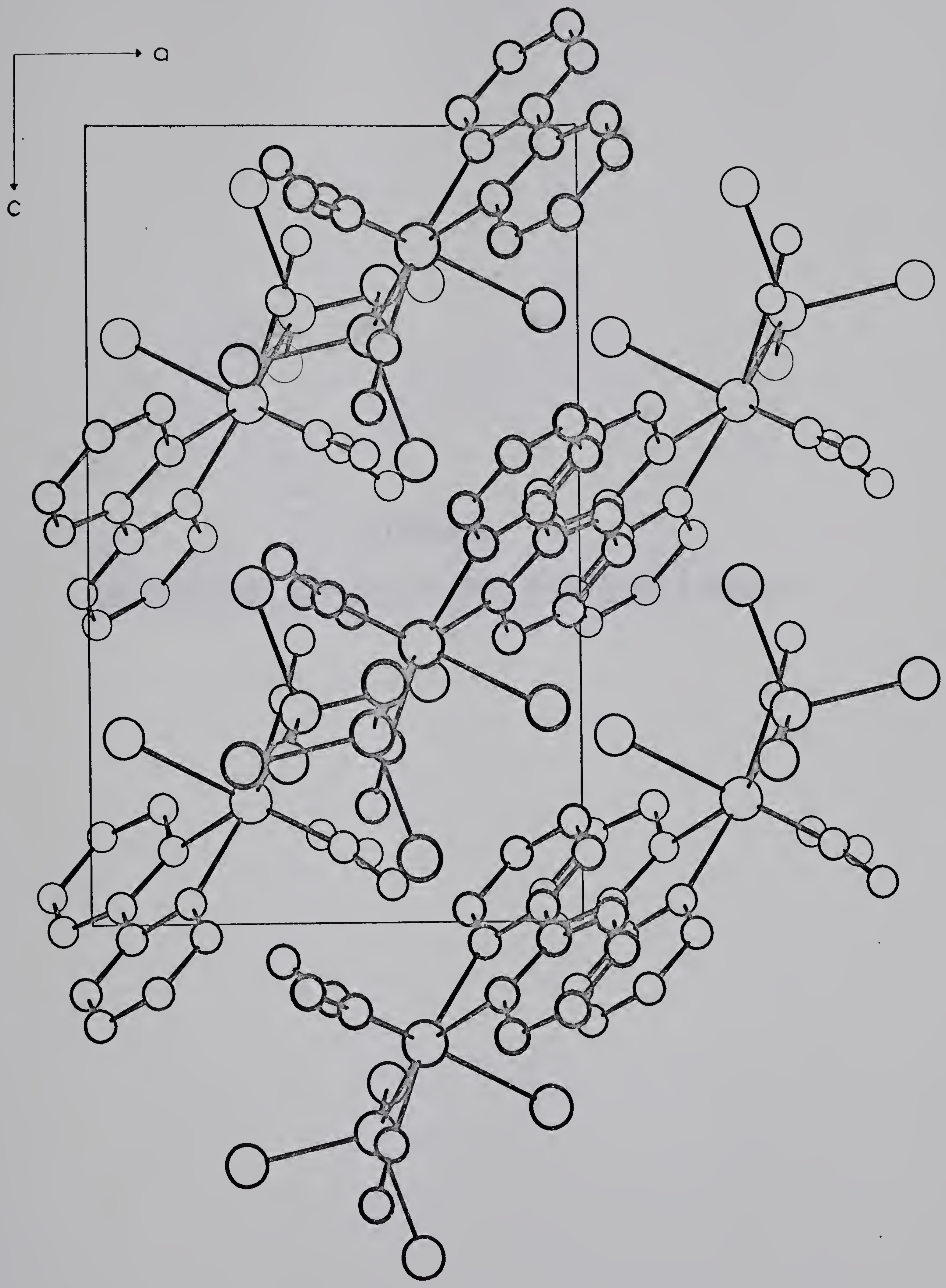
a
c

FIGURE 6

STEREOSCOPIC DIAGRAM OF THE MOLECULAR PACKING

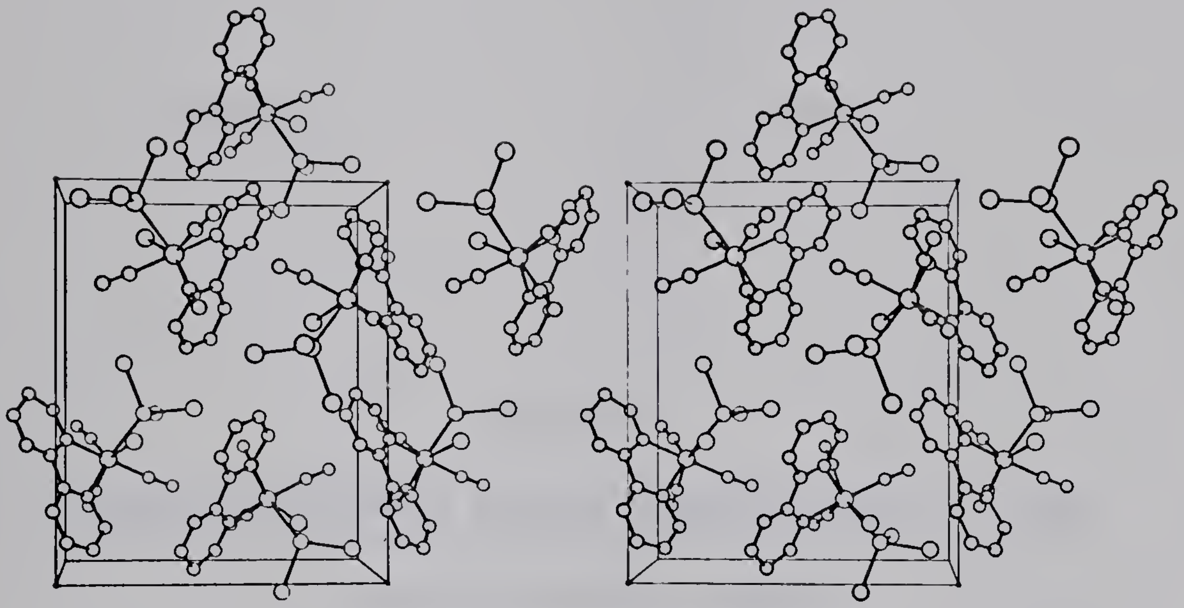

FIGURE 7

CAPPED TRIGONAL PRISM ARRANGEMENT OF THE
CO-ORDINATION ATOMS

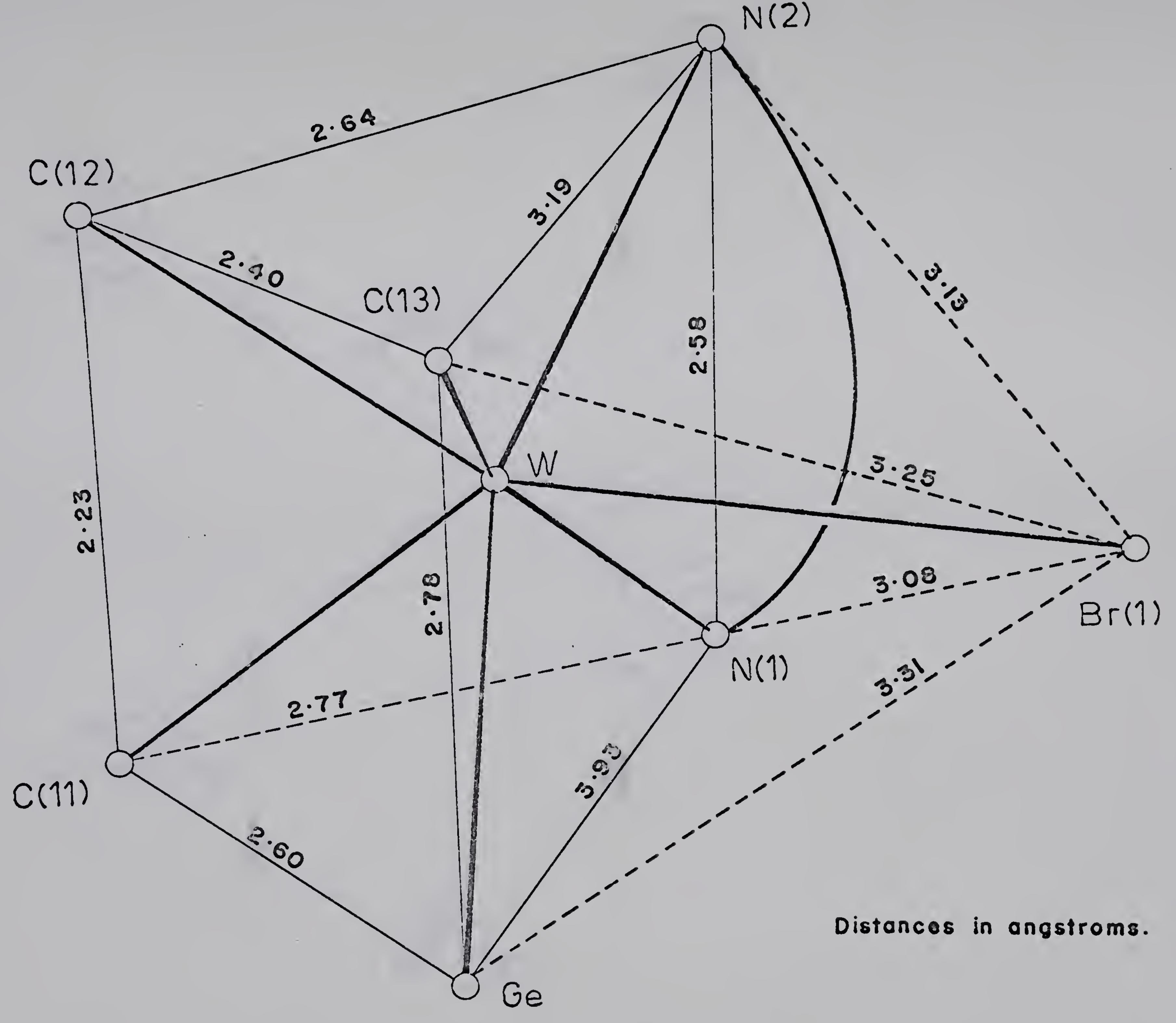
N(2)
C(12)
2·64
3·19
2·40
C(13)
2·58
3·13
3·25
W
2·23
2·78
3·08
Br(1)
N(1)
2·77
3·31
C(11)
3·93
2·60
Ge

Distances in angstroms.

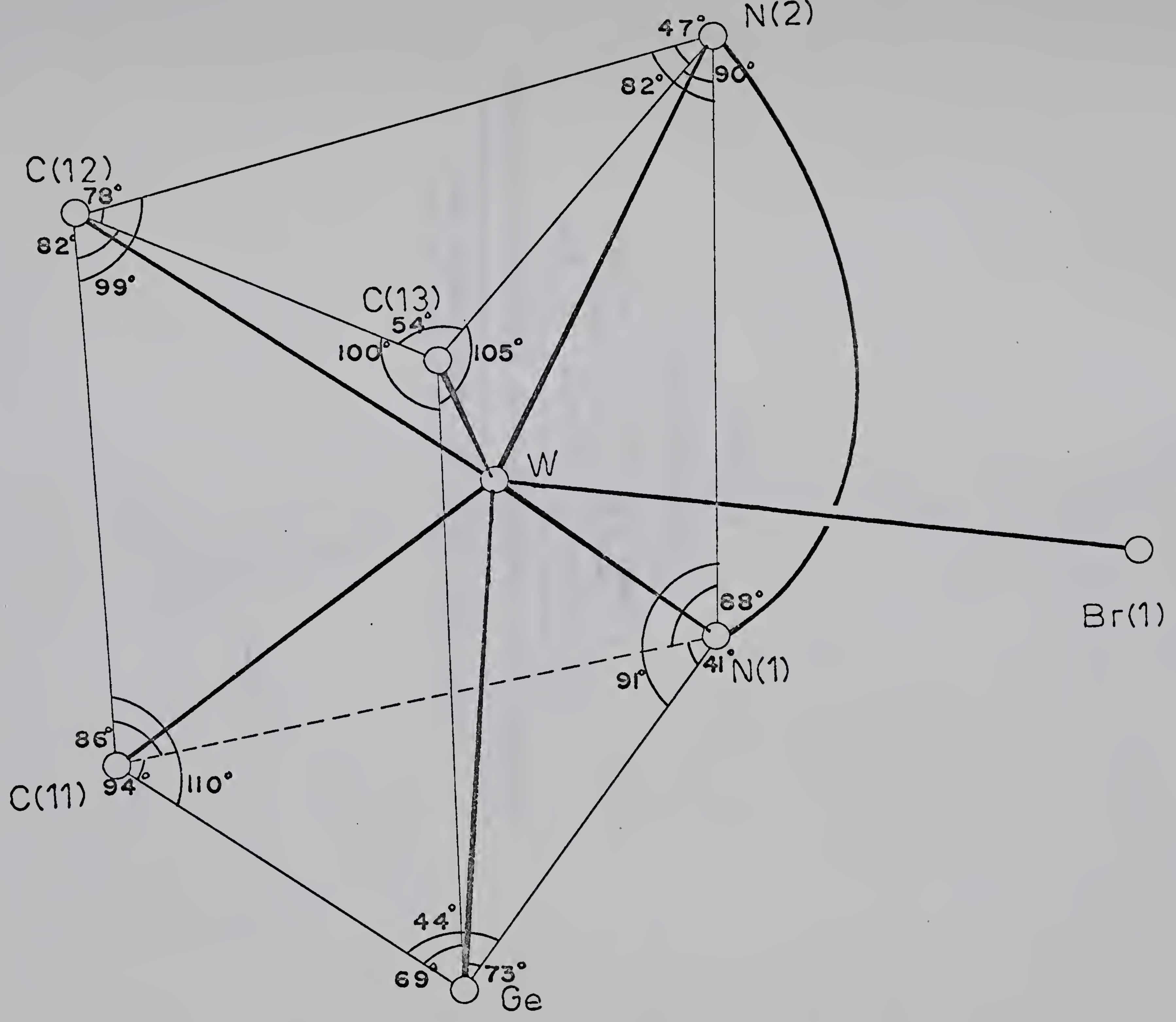
N(2)
47°
82°
90°
C(12)
78°
82°
99°
C(13)
54°
100°
105°
W
Br(1)
88°
91°
41°
N(1)
86°
94°
110°
C(11)
44°
69°
73°
Ge

FIGURE 8

APPROXIMATION OF

(a) $\mathrm{bipy(CO)_3BrWGeBr_3}$

and (b) $\mathrm{bipy(CO)_3C\ell MoSnCH_3C\ell_2}$

TO THE TETRAGONAL BASE-TRIGONAL BASE GEOMETRY

AS VIEWED DOWN THE FOUR-FOLD AXIS

(a)

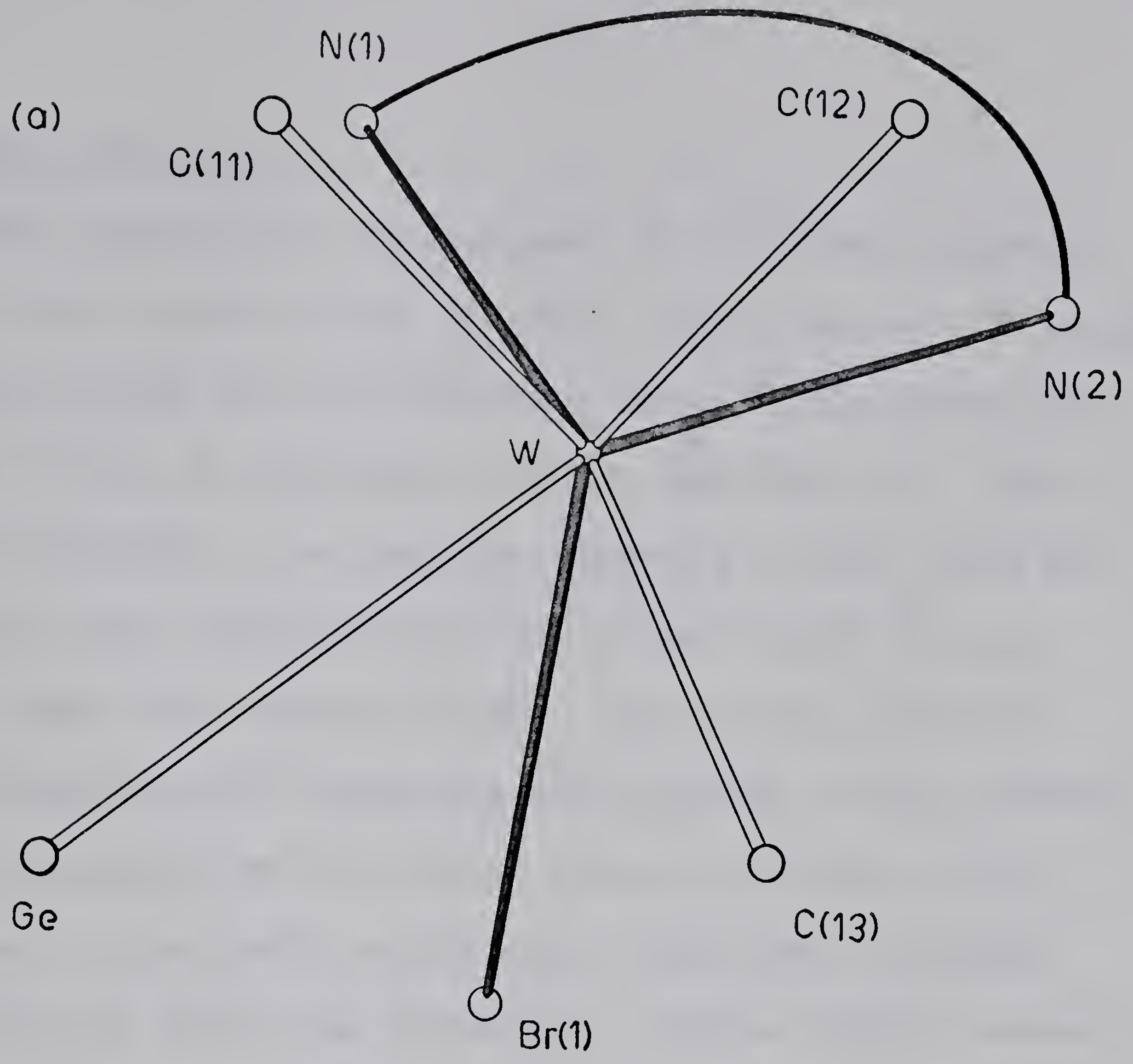
N(1)
C(11)
C(12)
N(2)
W
Ge
C(13)
Br(1)

(b)

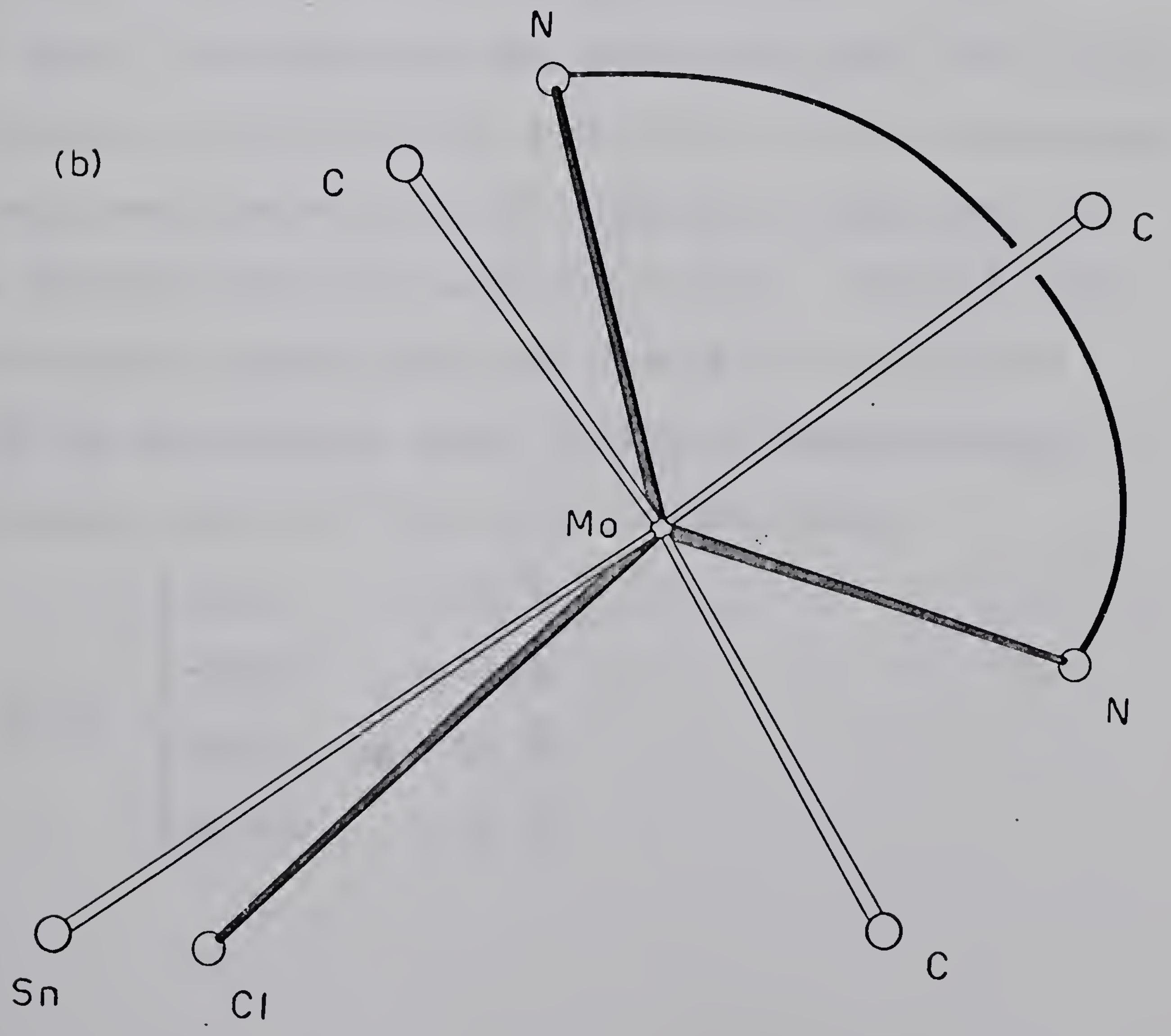
N
C
C
Mo
N
Sn
Cl
C

Molecular Geometry

The geometrical arrangement of the seven ligands around the tungsten atom closely approximates to a capped trigonal prism with the bromine atom, Br(1), above the centre of one of the square faces (see Fig. 7). The major distortion from regular geometry arises from the fact that the tungsten-germanium bond (2.608 Å) is longer than the tungsten-light atom bonds (∿2.0 Å) which comprise the remaining six ligands. This results in an expansion of the capped face (Ge, C(13), N(1), N(2)) and consequent reduction in the ideal trigonal prism angles about the germanium. These angles normally (60°, 90°, 90°) are (54°, 100°, 105°) about C(13), while about the germanium the values are (44°, 69°, 73°). The presence of the bromine atom, Br(1) above the capped face may contribute to the distortion of this face as it is observed that the edge N(2)-C(13) (3.19 Å) is significantly longer than that from N(2) to C(12) of 2.64 Å but the bromine atom, Br(1), is approximately equidistant from all four atoms in this face.

Br(1)	–Ge,	3.31 Å
	–N(1),	3.08 Å
	–N(2),	3.13 Å
	–C(13),	3.25 Å

The tungsten-germanium bond length is 2.608(6) Å which is the first recorded value for this type of bond. The sum of the covalent radii for germanium and tungsten, assuming values of 1.22 Å.[9a] for the tetrahedral covalent radius of germanium and 1.58 Å for the covalent tungsten radius, as found in $\pi C_5H_5W(CO)_3\sigma C_6H_5$,[10] is 2.80 Å and this value is somewhat larger than that observed. Alternatively by using the W-Br(1) bond length of 2.603 Å from this compound (assuming that halogens have essentially no π bonding character and that the Br radius is 1.14 Å [18]), a tungsten covalent radius of 1.46 Å is implied, and this predicts a slightly different tungsten-germanium bond length of 2.68 Å, which agrees more favourably with that observed. If this latter assumption of the covalent radius of tungsten is correct then the agreement between the observed and calculated values for the tungsten-germanium bond length suggests pure single bond character for this bond, although further measurements would be needed to confirm this deduction.

The germanium atom exhibits normal sp^3 hybridization with slight distortions in geometry arising from steric differences between the bromine ligands, Br(2), Br(3), Br(4) and the tungsten. As a result there is a contraction of the tetrahedral face involving the three

bromine atoms such that the average bromine-germanium--bromine angle is 100° compared to an average value of 117° for tungsten-germanium-bromine angles. None of the germanium-bromine bond lengths are significantly different from the others or from that reported for $GeHBr_3$, 2.298(3).[11] (Two bond lengths are said to be significantly different when the difference between them is in the order of 3σ where σ is the standard deviation of the mean value.) While the distance between the germanium atom and Br(1), 3.31 Å, is markedly shorter than the sum of the van der Waals radii, 3.95 Å, for these atoms, (calculated using a value of 1.95 Å for bromine,[9b] and 2.0 Å for germanium. The latter is assumed to have the same van der Waals radius as selenium and arsenic.)[9b], the more or less regular tetrahedral co-ordination of the germanium precludes any interaction of the type suggested for the corresponding contact in $\mathrm{bipy(CO)_3C\ell MoSnCH_3C\ell_2}$[6] where considerable distortions of the tin atom sp^3 hybridization result in approximate pentagonal bipyrimid (dsp^3) geometry.

Comparisons of the bonds and angles of the 2,2'-bipyridyl ligand in this compound with other reported values is not justified in view of the magnitude of the errors involved. Values of 1.40 Å, 1.36 Å, and 1.48 Å have been predicted for the $\mathrm{C}\overset{\cdots}{-}\mathrm{C}$, $\mathrm{C}\overset{\cdots}{-}\mathrm{N}$, $\mathrm{C{-}C}$ bonds respectively[12] and values closely approximating

to these have been observed in a number of complexes, namely trimethylacetylacetonyl 2,2'-bipyridyl Pt[13] and $(\mathrm{bipy})_2\mathrm{CuI}^+\mathrm{I}^-$.[14] No such trend is evident in this compound where average values for $\mathrm{C}\overset{\cdots}{-}\mathrm{C}$, $\mathrm{C}\overset{\cdots}{-}\mathrm{N}$, $\mathrm{C}-\mathrm{C}$ (1.41 Å, 1.41 Å, 1.44 Å) are not significantly different. The deviations from planarity for the 2,2-bipyridyl group are not significant since they are half the magnitude of the associated e.s.d's. With the twelve atoms included the equation of the least squares plane is

$$0.5968x + 0.3867y + 0.7031z - 6.5306 = 0 \ ,$$

the tungsten atom being positioned 0.29 Å above the plane.

The average tungsten-carbon and carbon-oxygen bond lengths of 1.92 Å and 1.19 Å respectively are not significantly different from corresponding bond lengths in $\mathrm{dithi(CO)_3C\ell WSnCH_3C\ell_2}$[6] of 1.96 Å and 1.16 Å or Mo-C (1.98 Å) and C-O (1.14 Å) bond lengths in $\mathrm{bipy(CO)_3C\ell MoSnCH_3C\ell_2}$.[6]

Discussion

The purpose of this crystal structure determination was to establish the difference, if any, between the hepta co-ordinate geometry of this compound, bipy$(CO)_3BrWGeBr_3$, and that of bipy$(CO)_3C\ell MoSnCH_3C\ell_2$.

It appears that the most obvious difference concerns the halogen bonded to the transition metal atom: in the latter this is bridging the molybdenum-tin bond while in this compound it is attached only to the tungsten atom. The overall description of the hepta-co-ordinate geometry has been given as distorted capped trigonal prism for the tungsten atom and distorted capped octahedron for the molybdenum atom in their respective compounds. An alternative way of describing these compounds is by the less conventional tetragonal base-trigonal base geometry which gives a better idea of the similarity of their geometries. It has already been suggested[15] that capped trigonal prism geometry approximates to the tetragonal base-trigonal base geometry (ii) (Table I, p. 5) and the capped octahedral arrangement, after considerable symmetrical distortion, resembles the tetragonal base-trigonal base geometry (i). Figure 8 shows the approximation of bipy$(CO)_3BrWGeBr_3$ (a) and bipy$(CO)_3C\ell MoSnCH_3C\ell_2$ (b) to this geometry.

In Figure 8(a) it can be seen that the vertical mirror plane is only approximate in the sense that Ge

is not equivalent to C(13), and further that N(1), C(12) and C(11), N(2) should be mirror related. i.e. the 'ideal' vertical symmetry plane would bisect the N(1)-N(2) and C(11)-C(12) edges and encompass Br(1). In contrast, the bipy$(CO)_3Cl MoSnCH_3Cl_2$ geometry shows a much closer approximation to mirror symmetry (Fig. 8(b)) which relates the two identical halves of the 2,2'-bipyridyl group and two of the three carbonyls. It is evident then that the difference between the two geometries may be considered as a difference in the orientation of the ligands related by the three-fold axis with respect to those related by the four-fold axis. More specifically if the three atoms N(1), N(2), Br(1) related by the three-fold axis (Fig. 8(a)) are rotated by ∿30° (clockwise), a ligand arrangement similar to that observed for bipy$(CO)_3Cl MoSnCH_3Cl_2$ (Fig. 8(b)) will result. By considering only steric interactions, the rotation of these three atoms will effect no change in the positions of the other four ligands Ge, C(11), C(12), C(13). Thus the two geometries are related by an apparently simple rotation of the trigonal face.

The adoption of one or other of these two configurations is undoubtedly dependent upon the ability of the tin or germanium atom to increase its co-ordination number, as well as the electronic and steric properties

of the (potentially bridging) halogen atom involved. In view of these facts the different structures adopted by bipy(CO)$_3$BrWGeBr$_3$ and bipy(CO)$_3$CℓMoSnCH$_3$Cℓ_2 are not surprising. For a particular compound in this series, in which the combination of group IV metal and halogen precludes an obvious choice, then presumably either one of the two configurations or both (in solution) might exist. Furthermore in view of the apparently facile convertability of the two forms there seems no obvious reason for discounting the possibility of the existence of both forms. If these two forms do in fact exist for a particular molecular species, then they will be geometrical isomers. The existence of similar geometrical isomers has been established for the heptaco-ordinate polyhedra $S_2Fe_3(CO)_9$ in the crystalline state. One form[15] is analogous to the bipy(CO)$_3$CℓMoSnCH$_3$Cℓ_2 arrangement of ligands and the other[16], which crystallizes with the molecular species $S_2Fe_2(CO)_6$, is analogous to this compound, bipy(CO)$_3$BrWGeBr$_3$. This illustrates the feasibility of such interconversions although this process is probably dependent on the nature of the ligands involved.

Whether the existence of such isomers in the series of compounds under study could explain the chemical and

infrared evidence of Kummer and Graham is open to question and so the possibility must remain that these proposed isomers are not necessarily representative of those observed for a particular species in solution.

THE CRYSTAL STRUCTURE OF TETRAETHYLAMINEPLATINUM II TETRACHLOROPLATINATE II,

($[Pt(etNH_2)_4][PtC\ell_4]$)

Introduction

The crystal structure of Magnus' green salt (abbreviated to MGS) shows it to be a chain structure of alternating parallel, square planar $PtC\ell_4^{2-}$ and $Pt(NH_3)_4^{2+}$ ions with a Pt···Pt separation in the direction of the chain of 3.25 Å.[19] Although this compound is green in the crystalline state, its constituent cations and anions are colourless and pink respectively. The abnormal colour and associated dichroism* which these crystals exhibit is attributed to the existence of weak bonds between adjacent platinum atoms.[20,23] This interpretation was questioned by Miller[22] who found compounds of the series $[MA_4][M'X_4]$, where M,M' ≡ Pt, Pd, Cu; A ≡ ammonia methylamine and various higher amines and X ≡ $C\ell^-$, Br^-, I^-, to be isomorphous and hence isostructural with MGS

---

* The absorption of light with its electric vector perpendicular to the ionic planes is at a lower frequency and more intense than that of light with its electric vector parallel to the planes. Usually the reverse occurs in the spectra of planar molecules.[22]

but only abnormally coloured when M and M' were platinum. Since no 'abnormality' was observed in compounds involving the following combinations of metals: Pd···Pd, Pt···Pd and Cu···Pt, all of which had metal-metal separations close to that observed in MGS, it was claimed that the association of 'abnormal' colour with metal-metal bonds in Pt···Pt compounds is incorrect and that the MGS-type structure is an electrostatically favourable one for square planar cations, MA_4^{2+}, and anions, MX_4^{2-}, to adopt without metal-metal interaction.

Yamada has subsequently demonstrated[24,26] that in compounds such as $[Pd(NH_3)_4][PdC\ell_4]$ the absorption spectra and dichroism are in fact 'abnormal' in a similar way to those of MGS (MGS shows an absorption band at ∿500 mμ which is not observed with either constituent ion) and this would appear to demonstrate the danger of basing arguments on colour rather than absorption spectra. In particular, a spectral study[23] of a number of higher amine analogues of MGS showed that while $[Pt(meNH_2)_4][PtC\ell_4]$ is green and has optical properties similar to MGS the ethylamine analogue is pink and shows bands in its absorption spectrum characteristic of its constituent ions. An explanation was given by Yamada et al. who suggested that the larger alkyl groups "sterically hinder" the chain structure and

prevent metal-metal bonding and hence the colour phenonenon. On further investigation Yamada[27] found that this change of properties with length of alkyl group does not occur, as compounds in similar series: $[PtA_4][PtBr_4]$ and $[PtA_4][PtI_4]$ are all 'abnormal' and thus it was deduced that an 'electronic factor' as well as a steric factor was operative in the formation of these complexes.

The results of a three dimensional crystal structure analysis, done by K. Phillips[28] in this laboratory, indicate that $[Pt(meNH_2)_4][PtC\ell_4]$ does have a structure analogous to MGS; it comprises chains of square planar anions and cations, the latter being swastika shaped as shown below.

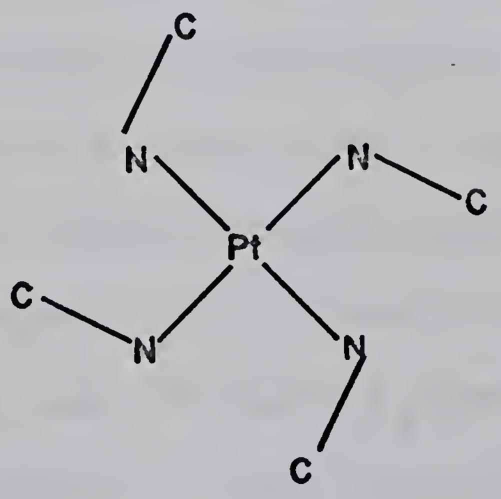

There appears to be no obvious reason why ethylamine or a higher amine should not form a planar cation, similar to that above, which could pack with the $PtC\ell_4^{2-}$ anion to form the MGS-type structure, as indeed this is

presumably what happens in the bromo and iodo platinates. It was apparent that a more detailed knowledge of the structures of these compounds would be of value and so tetraethylamineplatinum II tetrabromoplatinate II, $[Pt(etNH_2)_4][PtBr_4]$ and tetraethylamineplatinum II tetrachloroplatinate II, $[Pt(etNH_2)_4][PtC\ell_4]$ were structurally investigated.

Experimental

Tetraethylamineplatinum II tetrabromoplatinate II

Fine green tetragonal needles of $[Pt(etNH_2)_4][PtBr_4]$ were prepared by mixing aqueous solutions of $Pt(etNH_2)_4Br_2$ and K_2PtBr_4. Weissenberg photographs of layers hk0 and hk1 showed 4/mmm diffraction symmetry and systematically absent reflections were observed for $0k\ell$ with $k + \ell$ odd and $hh\ell$ with ℓ odd. Also $hk\ell$ reflections with h+k odd were systematically weak. These observations consistent with space groups P4nc or P4/mnc are similar to those for MGS, and $[Pt(meNH_2)_4][PtC\ell_4]$. The following table gives the unit cell dimensions for the three compounds

	[a]Å	[c]Å
$[Pt(NH_3)_4][PtC\ell_4]$	9.03	6.49
$[Pt(meNH_2)_4][PtC\ell_4]$	10.32	6.58
$[Pt(etNH_2)_4][PtBr_4]$	12.27	6.71

and as expected the [a] axis increases with the size of the amine ligand. It is obvious that $[\mathrm{Pt(etNH_2)_4}][\mathrm{PtBr_4}]$ has the same structure as MGS with chains of alternating parallel square planar $\mathrm{Pt(etNH_2)_4^{2+}}$ and $\mathrm{PtBr_4^{2-}}$ ions separated by 3.35 Å.

Tetraethylamineplatinum II tetrachloroplatinate II

Crystals of tetraethylamineplatinum II tetrachloroplatinate II, $[\mathrm{Pt(etNH_2)_4}][\mathrm{PtC\ell_4}]$ were prepared according to Reihlem and Flohr[25] by mixing equimolar quantities of aqueous solution of $\mathrm{K_2PtC\ell_4}$ and $\mathrm{Pt(etNH_2)_4C\ell_2}$. The fine pink precipitate which formed immediately, gave tiny pink needles on recrystallization from dilute $\mathrm{HC\ell}$. Analyses are as follows

$\mathrm{K_2PtC\ell_4}$	% Found Cℓ, 33.64 % Calc. Cℓ, 34.0
$\mathrm{Pt(etNH_2)_4C\ell_2}$	% Found C, 19.84; N, 11.40; H, 6.77 % Calc. C, 21.5; N, 12.6; H, 6.3
$[\mathrm{Pt(etNH_2)_4}][\mathrm{PtC\ell_4}]$	% Found C, 13.72; N, 8.17; H, 4.18 % Calc. C, 13.5; N, 7.9; H, 3.9

These needles are elongated in the [c] direction and exhibit very poorly developed faces. Their tendency to cleave parallel to the needle axis is a characteristic property of compounds with chain like structures.

After examining many crystals from several preparations a non-multiple crystal was found which was used for data collection. It had dimensions (0.034 x 0.034 x 0.086) mm along [a], [b] and [c] respectively. The unit cell and space group were determined from precession, rotation and Weissenberg photographs and the density was measured by flotation in a solution of dibromomethane and iodoform. Intensity data for the layers $0k\ell$, $1k\ell$, $2k\ell$, $3k\ell$ were recorded (with Cu Kα radiation) on Weissenberg photographs using the multiple film technique. Two exposures of 5 hrs. and 24 hrs. per layer were necessary to obtain measurements for all observed reflections. Each reflection was measured visually by comparison with a previously prepared scale which had a barely visible reflection for its unit. Corrections for Lorentz and Polarization effects were applied to the 500 observed reflections. No cross-axis data was collected for the purpose of interlayer scaling because of the difficulty in obtaining single crystals. Thus each layer was initially assigned a scale factor of 1.0 which was refined in subsequent calculations by comparison of observed and calculated structure factors.

During the early stages of photography weak reflections requiring [a] to be doubled, were observed on a long exposure rotation photograph. However, it was

assumed that they would not be of immediate significance in the structure determination as only a few were visible on a first weak layer Weissenberg film exposed for 80 hrs. After exclusion of these weak reflections, the crystal was most conveniently described in terms of a C-centred lattice and all constants pertaining to this cell are given in Table 9(a) (p. 64).

Structure Analysis

If the formula of the pink salt is taken as $[Pt(etNH_2)_4][PtC\ell_4]$ there is only one molecule per unit cell which obviously does not satisfy the requirements of a C-centred lattice. Thus it appeared the compound would be more correctly formulated as $Pt(etNH_2)_2C\ell_2$ and was not of the same type as MGS. The space group consideration of C1 and $C\bar{1}$ require the two equivalent platinum atoms be located at (0,0,0) and (½,½,0).

Using the centrosymmetric space group, $C\bar{1}$, structure factors were calculated on the basis of the platinum atom contribution only, and this resulted in a discrepency index, R, of 0.13 where $R = \Sigma||F_o| - |F_c||/\Sigma|F_o|$; F_o and F_c are the observed and calculated structure factors. A difference Fourier map phased by the platinum atom revealed the chlorine atom positioned along the [b] axis but after refinement by least squares methods using the

block diagonal approximation the isotropic temperature factor of this atom, initially 4.0 $\mathring{A}^2$, converged at a relatively high value of 9.0 $\mathring{A}^2$. This prompted the change from space group $C\bar{1}$ to C1 allowing a cis arrangement of ligands rather than trans but as no support was found for this change (every peak in the C1 difference Fourier, phased with the platinum and chlorine atoms, had a centrosymmetrically related peak of identical height) the centrosymmetric space group $C\bar{1}$ was retained. A three dimensional model of the peaks within a 4$\mathring{A}$ radius of the platinum atom showed two sets of square planar peaks rotated by 45° with respect to each other in the plane containing them. The approximate ratio of the peak heights of these two sets, 2:1, suggested a $PtC\ell_4^{2-}$ ion superposed on a $Pt(etNH_2)_4^{2+}$ ion forming a disordered packing arrangement, and thus the co-ordinates of appropriate peaks were assigned to all light atoms with the exception of the terminal carbon atoms of the ethylamine chains. A structure factor calculation with these atoms included and B_{iso} = 1.2 $\mathring{A}^2$ for the platinum atom, B_{iso} = 3.5 $\mathring{A}^2$ for the chlorine atom, B_{iso} = 4.0 $\mathring{A}^2$ for the nitrogen and carbon atoms gave an R factor of 0.089 (the occupancy factor of 0.5 was used for heavy and light atoms). Several cycles of full matrix least

squares refinement were calculated in which all positional parameters (except those of the platinum atom), isotropic temperature factors and scale factors were varied. From the small shifts in parameters (except for the temperature factor of Cℓ(2) which was positioned along the [a] axis and had a high correlation with the scale factors), it appeared that all the light atoms were genuine.

It became obvious that the observed disorder in packing was due to the fact that the repeating unit was a sub-cell of the true unit. In other words the weak reflections, previously disregarded, were important in distinguishing between the two different sorts of platinum atoms, namely $\mathrm{Pt(etNH_2)_4^{2+}}$ and $\mathrm{PtC\ell_4^{2-}}$ and as a first step to removing this disorder, the first weak layer was measured and processed in the same manner as the rest of the data. After inclusion of these weak reflections a new unit cell was found which was B-centred and derived from the reduced cell (Table 9(a)) by doubling the [a] and [c] axes. All constants pertaining to this B-centred cell are given in Table 9(b). The importance of the weak layer can now be realized as platinum atoms at (0,0,0) and (½,0,0) will not contribute to reflections of the type (1kℓ), which are therefore due only to the

light atoms e.g. considering only the trigonometric part of the structure factor expression for $B\bar{1}$:

$$F_{hk\ell} = \cos 2\pi(hx + ky + \ell z)\cdot\cos^2 \pi/2(h+\ell)$$

for the platinum atom at (0,0,0) $F_{hk\ell} = \cos 2\pi(0)\cdot 1 \quad = +1$

for the platinum atom at (½,0,0) $F_{hk\ell} = \cos 2\pi(h.\tfrac{1}{2})\cdot 1 = \cos\pi(h)$

and for h odd $F_{hk\ell} = -1$

i.e. the contribution from the platinum atom at (0,0,0) exactly cancels that at (½, 0,0)

The data was accordingly transformed to the new space group using the transformation matrix below.

$$\begin{pmatrix} 2 & 0 & 0 \\ -\tfrac{1}{2} & \tfrac{1}{2} & 0 \\ 0 & 0 & 2 \end{pmatrix}$$

The matrix used to transform the atomic co-ordinates from the C-centred to the B-centred cell is

$$\begin{pmatrix} \tfrac{1}{2} & \tfrac{1}{2} & 0 \\ 0 & 2 & 0 \\ 0 & 0 & \tfrac{1}{2} \end{pmatrix}$$

The terminal carbon atoms of the ethylamine chains were located without difficulty from a $B\bar{1}$ difference Fourier map (phased by the other atoms) and several refinement cycles using full matrix least squares in

which scale factors and other parameters were varied alternately, resulted in convergence at R = 0.078. The discrepency index of the 36 weak reflections for the layer 1kℓ was 0.116 and $R_w = \{\Sigma w[|F_o| - |F_c|]^2/\Sigma w|F_o|^2\}^{\frac{1}{2}} = 0.108$ where $w = a^2/(a^2 + (F_{obs} - b)^2)$, with a = 50 and b = 15.

The final difference map showed quite a number of fluctuations in electron density, the largest being either side of the platinum positions, which is indicative of anisotropy in the platinum atom or absorption errors. Most of the other features appeared to be random and could be attributed largely to the lack of cross-axis data and absorption effects which were not corrected for. It has been shown that positional parameters are not affected to any great extent when absorption corrections are not made but temperature factors may alter considerably.[29] The scattering factors used for platinum, chlorine, nitrogen and carbon, with a real anomalous dispersion correction for platinum, are from the International Tables.[7]

Results

The observed and calculated structure factors are listed in Table 10 and are on the absolute scale x 10. Table 11 gives the final atomic co-ordinates and isotropic temperature factors. Estimated standard deviations obtained from the inverse matrix of the final least squares refinement cycle are given in parentheses beside parameters in all tables. The large magnitudes of the standard deviations associated with light atom parameters demonstrate the difficulty in locating light atoms in the presence of very heavy ones. Tables 12, 13 and 14 list the intraionic distances, bond angles and selected interionic distances <4 Å. The configuration of the cation and anion with the atomic labelling scheme used is shown in Figure 9 with a prime symbol indicating the centrosymmetrically equivalent light atoms. The ionic packing in the plane perpendicular to the [c] axis and in the [a] [c] plane is shown in Figures 10 and 11 respectively.

TABLE 9

UNIT CELL DIMENSIONS

Tetraethylamineplatinum II tetrachloroplatinate II

$(C_8C\ell_4H_{28}N_4Pt_2)$

M.W. = 712.4 ρ_{obs} = 2.55 ρ_{calc} = 2.56

(a) Space group - C$\bar{1}$

	Reduced cell
[a] = 6.95 ± 0.01 Å	[a] = 6.95 Å
[b] = 18.58 ± 0.02 Å	[b] = 9.78 Å
[c] = 3.62 ± 0.01 Å	[c] = 3.62 Å
α = 98.8 ± 0.2°	α = 98.3°
β = 90.1 ± 0.2°	β = 90.1°
γ = 92.3 ± 0.2°	γ = 108.3°
V = 461.6 Å	V = 230.8 Å

z = 1 (i.e. two $PtC\ell_2(etNH_2)_2$ units)

Absences - hkℓ for h+k odd.

(b) Space group - B$\bar{1}$

	Reduced cell
[a] = 13.90 Å	[a] = 7.56 Å
[b] = 9.78 Å	[b] = 9.78 Å
[c] = 7.24 Å	[c] = 7.24 Å
α = 98.3°	α = 98.3°
β = 90.1°	β = 113.1°
γ = 108.3°	γ = 103.4°
V = 923.2 $Å^3$	V = 461.6 $Å^3$

z = 2

Absences - hkℓ for h+ℓ odd

TABLE 10

OBSERVED AND CALCULATED STRUCTURE FACTORS ON THE ABSOLUTE SCALE x 10

K	L	FO	FC
	H = 0		
0	4	1164	1039
0	6	699	673
0	8	533	452
1	4	1055	965
-1	4	1370	1253
1	6	778	767
-1	6	782	792
1	8	652	548
-1	8	582	527
2	2	1302	1386
-2	2	1067	959
-2	4	1100	1043
2	6	934	865
-2	6	824	842
2	8	636	546
-2	8	632	589
-3	2	1068	1049
3	4	1155	1066
-3	4	926	907
3	6	718	709
-3	6	749	788
3	8	543	469
-3	8	620	590
-4	0	1158	1369
4	2	922	1024
-4	2	1111	1307
4	4	758	753
-4	4	980	971
4	6	628	589
-4	6	689	717
4	8	556	441
-4	8	508	528
-5	0	1085	1113
5	2	881	835
-5	2	1100	1316
5	4	670	704
-5	4	998	1052
5	6	715	576
-5	6	643	737
-5	8	466	486
-6	0	934	908
6	2	919	855
-6	2	877	974
6	4	769	727
-6	4	800	943
6	6	734	543
-6	6	636	742
-6	8	403	504
-7	0	995	934
7	2	1034	904
-7	2	717	766
7	4	772	688
-7	4	547	640
7	6	621	476
-7	6	413	569
-7	8	437	461
8	2	890	749
-8	2	825	836
8	4	712	555
-8	4	527	629
-8	6	438	476
-9	0	580	615
9	2	606	530
-9	2	708	698
9	4	617	464
-9	4	708	661
-9	6	504	516
-10	0	518	484
10	2	633	450
-10	2	550	497
-10	4	524	524
-11	0	652	503
-11	2	533	473
-11	4	407	428
	H = 1		
0	3	83	-63
0	-3	231	-193
1	-1	195	-158
-1	1	144	-137
1	3	226	146
1	-3	293	-276
-1	3	290	-270
-1	-3	91	64
1	-5	251	-246
-1	5	203	-201
2	-1	114	-97
-2	1	164	-133
2	-3	130	-101
-2	3	238	-210
2	-5	158	-125
-2	5	225	-217
3	1	258	-278
3	-1	199	-213
-3	1	145	-147
-3	-1	149	-159
3	3	227	-240
3	-3	84	-55
-3	-3	171	-175
4	1	248	-293
4	-1	240	-269
-4	1	290	-315
-4	-1	287	-377
4	3	147	-148
4	-3	172	-158
-4	3	131	-118
-4	-3	232	-241
-5	1	152	-164
-5	-1	140	-145
-5	3	169	-147
	H = 2		
0	2	1144	1145
0	4	871	800
0	-4	1006	895
0	6	636	582
0	-6	669	617
0	8	451	450
0	-8	444	438
-1	-2	1132	1121
1	4	852	786
1	-4	1104	1021
-1	4	975	902
-1	-4	947	804
1	6	694	649
1	-6	833	744
-1	6	635	613
-1	-6	637	607
1	8	501	488
1	-8	480	495
-1	8	423	428
-1	-8	466	472
2	2	890	908
-2	2	1132	1131
-2	-2	1003	925
2	4	898	877
2	-4	908	804
-2	4	1024	975
-2	-4	896	801
2	6	702	680
2	-6	757	714
-2	6	744	736
-2	-6	737	666
2	8	478	456
2	-8	534	543
-2	8	501	502
-2	-8	501	497
3	0	984	1123
3	2	983	1096
3	-2	866	886
-3	2	734	723
-3	-2	968	950
3	4	835	835
3	-4	694	674
-3	4	798	742
-3	-4	920	892
3	6	606	567
3	-6	546	553
-3	6	673	693
-3	-6	698	677
3	8	415	387
3	-8	376	461
-3	8	523	538
-3	-8	476	452
4	0	967	1090
-4	0	1003	1148
4	2	800	821
4	-2	1060	1125
-4	2	896	929
-4	-2	984	1092
4	4	619	590
4	-4	896	879
-4	4	685	701
-4	-4	821	818
4	6	472	463
4	-6	609	605
-4	6	538	557
-4	-6	581	554
4	-8	356	423
-4	8	420	454
-4	-8	394	385
5	0	701	705
-5	0	899	1038
5	2	644	617
5	-2	745	818
-5	2	969	1113
-5	-2	773	783
5	4	555	572
5	-4	778	810
-5	4	831	907
-5	-4	592	582
5	6	524	500
5	-6	668	660
-5	6	576	629
-5	-6	524	470
-5	8	381	425
6	0	734	713
-6	0	699	710
6	2	776	727
6	-2	629	652
-6	2	679	808
-6	-2	654	638
6	4	720	639
6	-4	554	610
-6	4	699	799
-6	-4	608	596
6	6	528	481
6	-6	518	554
-6	6	620	653
-6	-6	587	514
-6	8	422	459
-7	0	771	750
7	2	749	690
7	-2	700	691
-7	2	610	673
-7	-2	773	753
7	4	649	535
7	-4	535	570
-7	4	504	597
-7	-4	794	647
7	6	446	384
7	-6	419	467
-7	6	457	529
-7	-6	556	490
-7	8	381	433
8	0	695	636
-8	0	763	762
8	2	627	535
8	-2	700	657
-8	2	672	696
-8	-2	731	689
8	4	487	426
8	-4	540	576
-8	4	516	560
-8	-4	639	531
8	-6	393	451
-8	6	379	446
-8	-6	430	383
9	0	561	498
-9	0	703	620
9	2	515	445
9	-2	550	542
-9	2	636	640
-9	-2	623	528
9	4	468	396
9	-4	531	531
-9	4	532	567
-9	-4	515	427
9	-6	415	450
-9	6	389	449
10	0	463	433
-10	0	529	481
10	2	474	475
10	-2	397	428
-10	2	532	516
-10	-2	508	443
10	-4	382	419
-10	4	484	515
-10	-4	460	401
-10	6	391	450
11	0	518	429
-11	0	435	434
11	-2	411	407
-11	2	390	424
-11	-2	483	426
-11	4	325	412
-12	0	477	431
-12	2	512	418
	H = 4		
0	2	922	872
0	-2	1219	1143
0	4	724	666
0	-4	1128	1049
0	6	582	566
0	-6	815	754
0	8	461	480
0	-8	513	471
1	0	958	1078
1	2	900	825
1	-2	1072	1027
-1	2	1086	1179
1	4	761	735
1	-4	964	898
1	6	672	659
1	-6	793	737
-1	6	651	627
1	8	487	492
1	-8	547	523
-1	8	841	435
2	0	1104	1162
2	2	1021	1037
2	-2	1129	1083
-2	2	1165	1099
-2	-2	918	796
2	4	890	864
2	-4	868	787
-2	4	1047	1050
-2	-4	795	641
2	6	700	621
2	-6	630	590
-2	6	843	780
-2	-6	604	575
2	8	395	404
2	-8	433	475
-2	8	515	491
-2	-8	518	497
3	0	1003	1116
3	2	1035	1044
3	-2	1025	1003
-3	2	1040	1000
-3	-2	973	891
3	4	783	763
3	-4	808	776
-3	4	894	846
-3	-4	876	771
3	6	562	500
3	-6	547	545
-3	6	719	716
-3	-6	746	654
3	-8	338	407
-3	8	520	533
-3	-8	518	470
4	0	936	949
-4	0	1075	1182
4	2	857	835
4	-2	865	869
-4	2	1049	1075
-4	-2	1053	1050
4	4	668	626
4	-4	741	753
-4	4	805	764
-4	-4	950	833
4	6	489	488
4	-6	579	598
-4	6	571	565
-4	-6	683	573
-4	8	403	464
-4	-8	401	376
5	0	702	704
-5	0	1025	1065
5	2	682	650
5	-2	680	715
-5	2	943	994
-5	-2	983	973
5	4	652	609
5	-4	642	678
-5	4	779	800
-5	-4	764	709
5	6	543	520
5	-6	586	607
-5	-6	543	477
6	0	653	635
-6	0	837	858
6	2	666	656
6	-2	585	623
-6	2	753	824
-6	-2	779	764
6	4	656	606
6	-4	503	581
-6	4	689	763
-6	-4	668	607
6	6	517	459
6	-6	485	511
-6	6	579	630
-6	-6	570	492
-6	8	345	444
7	0	682	692
-7	0	667	671
7	2	665	623
7	-2	681	678
-7	2	613	669
-7	-2	680	641
7	4	516	483
7	-4	592	593
-7	4	561	638
-7	-4	670	606
7	-6	417	462
-7	6	523	586
-7	-6	584	506
-7	8	403	469
8	0	653	596
-8	0	641	662
8	2	535	483
8	-2	675	636
-8	2	600	645
-8	-2	699	653
8	4	382	380
8	-4	602	586
-8	4	481	573
-8	-4	621	573
8	-6	442	469
-8	6	409	482
-8	-6	472	425
9	0	493	477
-9	0	702	668
9	2	442	431
9	-2	512	496
-9	2	633	677
-9	-2	660	578
9	-4	457	468
-9	4	542	600
-9	-4	479	442
-9	6	342	462
10	0	471	443
-10	0	587	548
10	-2	374	421
-10	2	562	587
-10	-2	501	455
10	-4	384	380
-10	4	545	556
-10	-4	356	372
-10	6	413	463
-11	0	431	458
-11	2	393	463
-11	-2	425	427
-11	4	377	437
-12	0	436	433
-12	2	400	413
	H = 6		
0	2	1012	900
0	4	911	784
0	-4	1251	1106
0	6	721	666
0	-6	847	787
0	-8	452	508
1	0	1148	1092
1	2	1195	1060
1	-2	1178	1047
-1	2	1240	1127
1	4	1049	903
1	-4	1021	939
-1	4	988	837
-1	-4	1144	978
1	6	735	678
1	-6	786	757
-1	6	687	635
-1	-6	733	676
1	-8	466	539
-1	-8	459	469
2	0	1296	1279
2	2	1281	1173
2	-2	1124	1059
-2	2	1332	1357
-2	-2	1172	1007
2	4	971	863
2	-4	860	791
-2	4	1144	1069
-2	-4	1028	786
2	6	624	579
2	-6	650	618
-2	6	946	733
-2	-6	778	640
-2	8	452	480
-2	-8	511	494
3	0	1231	1174
-3	0	1039	1063
3	2	1014	969
3	-2	1149	1113
-3	2	1274	1182
-3	-2	1093	933
3	4	761	709
3	-4	877	849
-3	4	1112	1065
-3	-4	1067	842
3	6	527	515
3	-6	587	601
-3	6	872	796
-3	-6	819	693
-3	8	466	526
-3	-8	508	500
4	0	877	848
-4	0	1138	1187
4	2	813	756
4	-2	909	907
-4	2	1123	1040
-4	-2	1281	1154
4	4	695	657
4	-4	853	843
-4	4	895	864
-4	-4	1066	926
4	6	483	529
4	-6	600	659
-4	6	744	693
-4	-6	724	654
-4	-8	446	434
5	0	703	720
-5	0	1267	1299
5	2	739	735
5	-2	661	697
-5	2	1014	1108
-5	-2	1227	1134
5	4	693	658
5	-4	660	682
-5	4	823	800
-5	-4	939	809
5	-6	515	607
-5	6	611	588
-5	-6	607	548
6	0	768	762
-6	0	1089	1053
6	2	691	707
6	-2	664	702
-6	2	973	1049
-6	-2	955	872
6	4	543	566
6	-4	478	596
-6	4	793	850
-6	-4	761	676
-6	6	531	615
-6	-6	569	522
7	0	698	691
-7	0	774	762
7	2	593	571
7	-2	627	716
-7	2	751	803
-7	-2	741	733
7	-4	470	616
-7	4	714	786
-7	-4	706	668
-7	6	563	653
-7	-6	546	536
8	0	459	541
-8	0	713	727
8	-2	497	592
-8	2	603	670
-8	-2	803	741
-8	4	589	634
-8	-4	702	641
-8	6	463	571
-8	-6	578	475
-9	0	807	762
-9	2	625	728
-9	-2	746	666
-9	4	521	607
-9	-4	497	513
-10	0	622	641
-10	2	692	698
-10	-2	473	520
-10	4	504	624
-11	0	459	505
-11	4	501	521
-12	0	452	468

FIGURE 9

CONFIGURATION OF CATION AND ANION WITH THE LABELLING SCHEME USED.

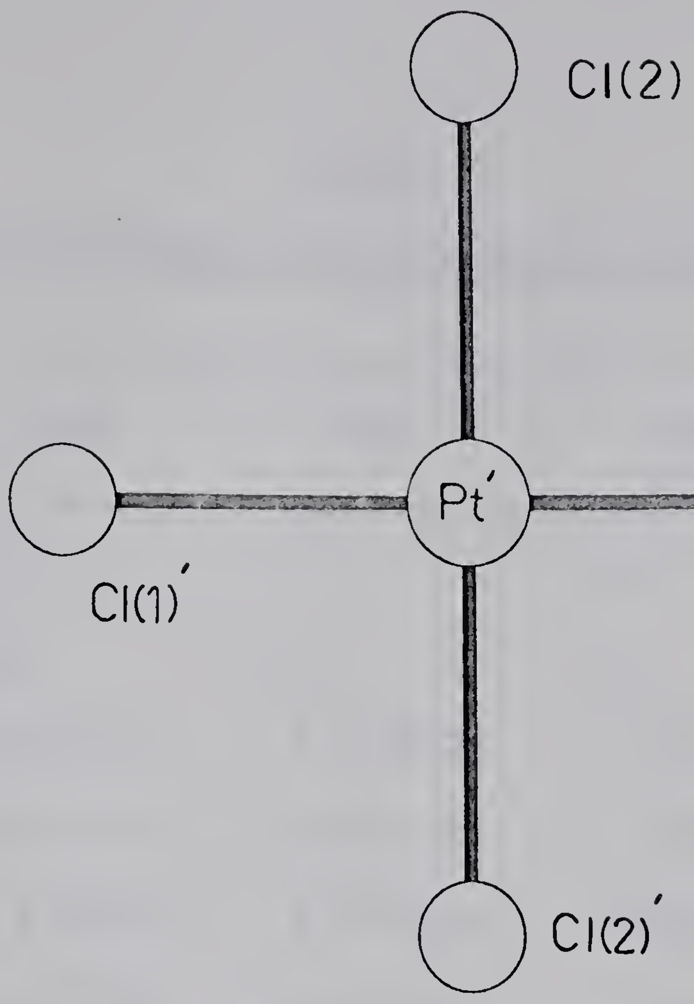
Cl(2)
Cl(1)′
Pt′
Cl(1)
Cl(2)′

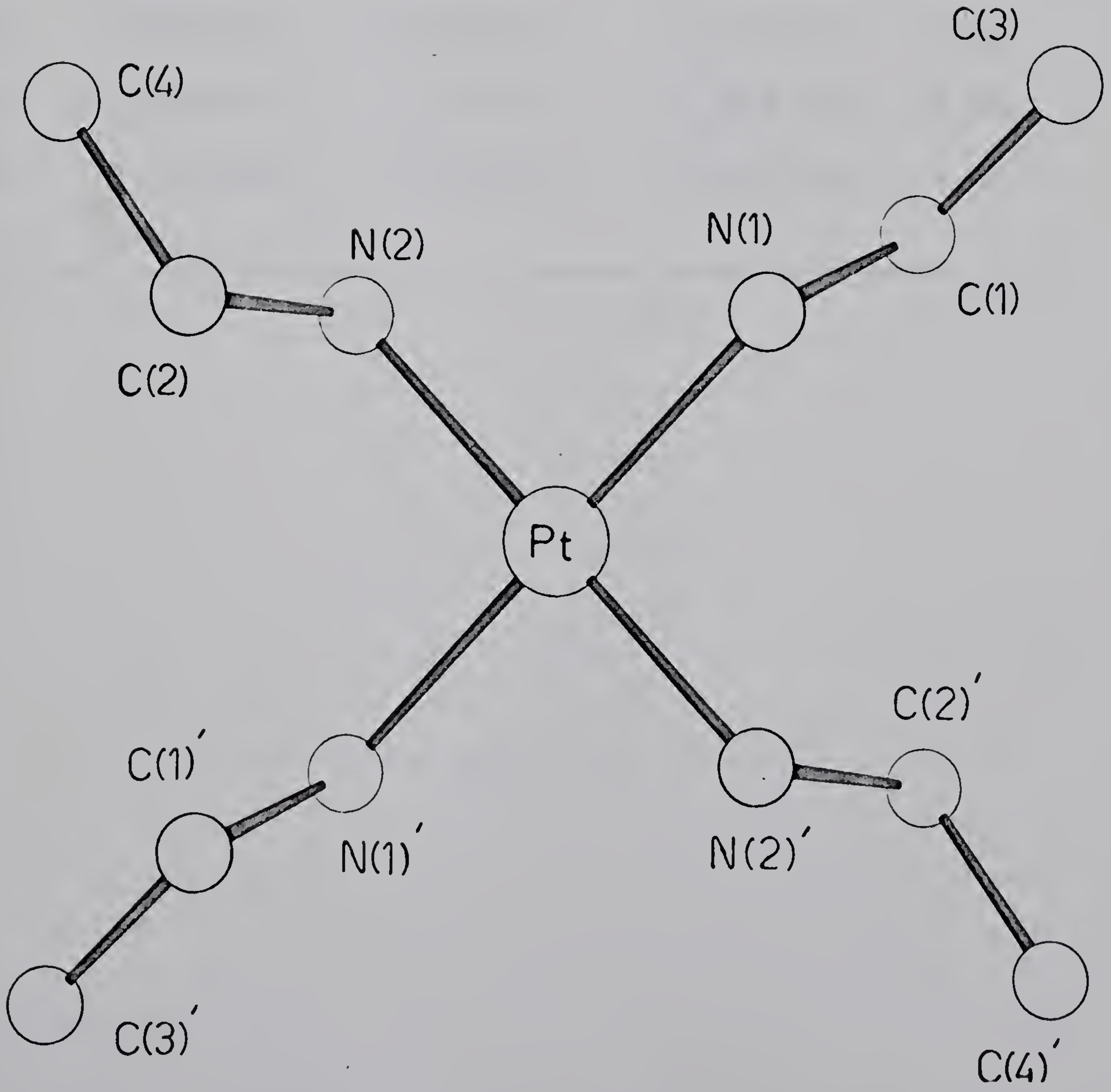
C(4)
C(3)
N(2)
N(1)
C(1)
C(2)
Pt
C(2)′
C(1)′
N(1)′
N(2)′
C(3)′
C(4)′

TABLE 11

ATOMIC CO-ORDINATES AND ISOTROPIC TEMPERATURE FACTORS

Atom	x/a	y/b	z/c	B_{iso}
Pt	0	0	0	1.6(1)
Pt'	0.5	0	0	0.9(1)
Cℓ(1)	0.555(3)	0.253(2)	0.072(2)	3.4(3)
Cℓ(2)	0.674(3)	0.001(1)	0.002(2)	3.8(3)
N(1)	0.136(8)	0.152(5)	-0.063(7)	4(1)
N(2)	0.072(8)	-0.146(5)	0.056(6)	4(1)
C(1)	0.193(11)	0.264(7)	0.119(10)	5(2)
C(2)	0.067(11)	-0.266(7)	-0.119(9)	5(2)
C(3)	0.288(17)	0.366(9)	0.048(12)	6(2)
C(4)	0.125(16)	-0.362(9)	-0.054(11)	6(2)

TABLE 12

INTRAIONIC DISTANCES

Atom A	Atom B	Bond lengths in Å
(a) Bonding		
Pt'	Cℓ(1)	2.33(1)
Pt'	Cℓ(2)	2.41(4)
Pt	N(1)	2.11(8)
Pt	N(2)	2.06(8)
N(1)	C(1)	1.61(9)
N(2)	C(2)	1.58(9)
C(1)	C(3)	1.53(20)
C(2)	C(4)	1.53(20)
(b) Non-bonding		
Pt	C(1)	3.10
Pt	C(2)	3.04
N(1)	C(2)	3.85
N(2)	C(1)	3.79
N(1)	C(3)	2.50
N(2)	C(4)	2.48

TABLE 13

BOND ANGLES

Atom A	Atom B	Atom C	Angle in degrees
Cℓ(1)	Pt'	Cℓ(2)	90(1)
N(1)	Pt	N(2)	93(3)
Pt	N(1)	C(1)	112(5)
Pt	N(2)	C(2)	112(5)
N(1)	C(1)	C(3)	105(6)
N(2)	C(2)	C(4)	105(7)

TABLE 14

SELECTED INTERIONIC DISTANCES LESS THAN 4 Å

Atom A	Atom B	Distance in Å	Symmetry transformation to be applied to Atom B		
Pt'	Pt	3.62	$\frac{1}{2}+x$	y	$\frac{1}{2}+z$
Pt'	N(1)	3.56	$\frac{1}{2}+x$	y	$\frac{1}{2}+z$
Pt'	N(2)'	3.60	$\frac{1}{2}+x$	y	$\frac{1}{2}+z$
Cℓ(1)	N(1)	3.27	$\frac{1}{2}+x$	y	$\frac{1}{2}+z$
Cℓ(1)	N(2)'	3.34	$\frac{1}{2}+x$	y	$\frac{1}{2}+z$
Cℓ(2)	N(1)	3.39	$\frac{1}{2}+x$	y	$\frac{1}{2}+z$
Cℓ(2)	N(2)	3.44	$\frac{1}{2}+x$	y	$\frac{1}{2}+z$
Cℓ(1)	C(1)	3.80	$\frac{1}{2}+x$	y	$\frac{1}{2}+z$
Cℓ(1)	C(2)'	3.72	$\frac{1}{2}+x$	y	$\frac{1}{2}+z$
Cℓ(2)'	N(1)	3.48	x	y	z
Cℓ(2)'	N(2)	3.43	x	y	z
Cℓ(2)'	C(1)	3.64	x	y	z
Cℓ(2)'	C(2)	3.73	x	y	z
Cℓ(2)'	C(3)	3.76	x	y	z
Cℓ(2)'	C(4)	3.72	x	y	z

FIGURE 10

IONIC PACKING IN PLANE PERPENDICULAR TO [c] AXIS

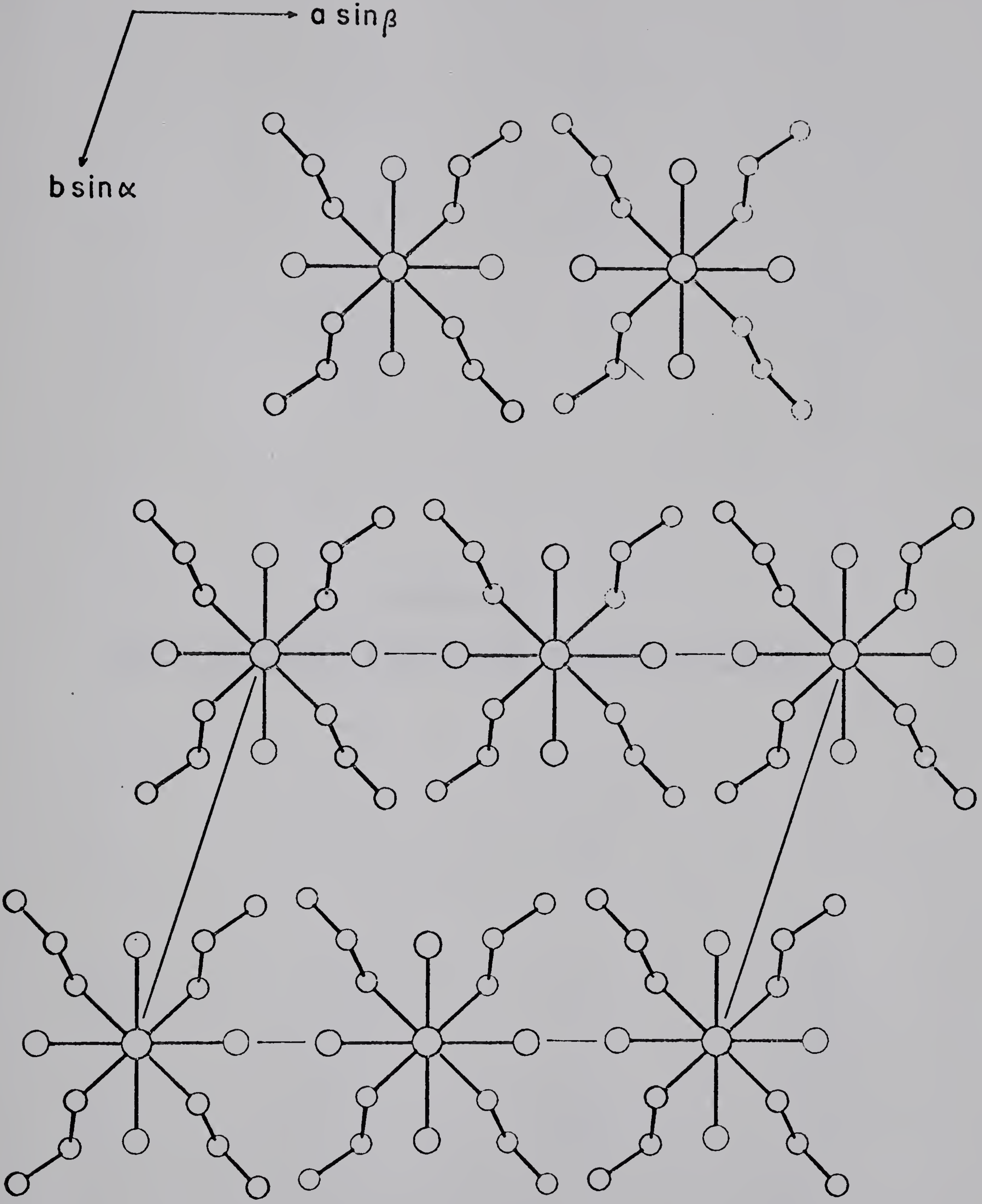
$a\sin\beta$
$b\sin\alpha$

FIGURE 11

IONIC PACKING - PROJECTION ONTO [a][c] PLANE

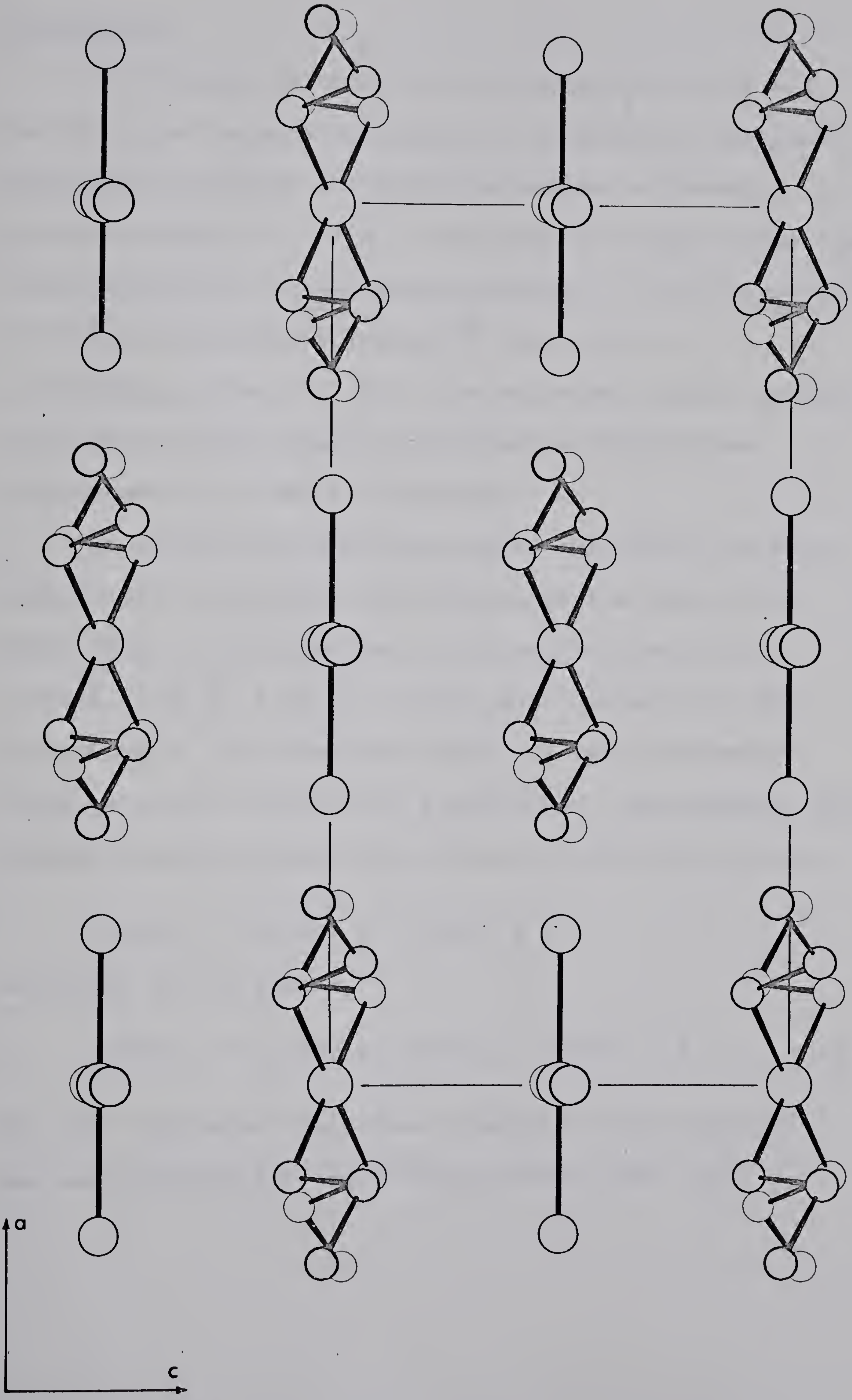
a
c

Discussion

The crystal structure of $[Pt(etNH_2)_4][PtC\ell_4]$ may be described as parallel chains of alternating cations and anions in which the distance between adjacent platinum atoms is 3.62 Å. (a somewhat larger value than that observed for other MGS-type salts: 3.25 Å in MGS,[19] 3.29 Å in $[Pt(meNH_2)_4][PtC\ell_4]$[28] and 3.35 in $[Pt(etNH_2)_4][PtBr_4]$). Both the anion and cation exhibit the square planar (dsp^2 hybridized) configuration characteristic of Pt II complexes.

In contrast to MGS-type salts, the cation in this compound is non-planar (deviations of the atoms C(1), C(2), C(3), C(4) from the co-ordination plane are 1.49 Å, 1.46 Å, 1.30 Å, 1.27 Å) which results in the reduction of the effective length of the ethylamine ligands in the [a] and [b] directions. Furthermore, the dihedral angle between the cation co-ordination plane:

$$0.0103x + 0.2827y + 0.9592z = 0$$

and that of the anion:

$$0.0050x + 0.2199y - 0.9755z - 0.0347 = 0 \qquad \underline{A}$$

of 151° indicates that these planes are not parallel as was observed for the MGS-type salts (Fig. 11).

It is obvious that this distortion, which may be considered as a rotation of the cation by ∿30° with respect to the anion about the [a] axis, could result in greater interaction between atoms of neighbouring cations and anions. Undoubtedly, these potentially large steric interactions are reduced by the "staggering" of the ions (Fig. 10) i.e. rotation of the cation by ∿45° with respect to the anion about the [c] axis, which also occurs in MGS-type compounds but to a lesser extent. A plausible explanation for the non-parallel nature of the ion co-ordination planes can be found by considering the least squares plane through all atoms of the cation; this plane:

$$0.0017x - 0.0919y - 0.9958z = 0$$

is approximately parallel to the anion plane (equation A) giving a dihedral angle of 173°. Clearly the rotation of the cation co-ordination plane minimises the 'space' utilised by the cation to allow more efficient packing along the [c] axis i.e. in the chain direction. The ionic packing in this compound may now be described as essentially similar to that of MGS but with its non-planar cations occupying more 'space' in the chain direction (Fig. 11) than the planar MGS-type cations. Thus it seems that electrostatically favourable packing has been

maintained despite the non-planarity of the ethylamine cation.

By considering the structural differences between this compound and MGS-type salts it seems probable that the reason for the lack of Pt···Pt interaction in the former, lies not in the larger metal-metal separation but rather in the mutual orientation of the cation and anion co-ordination planes. These are not parallel, nor perpendicular to the line joining the platinum atoms and if it is assumed that the Pt···Pt interaction involves overlap of axial metal orbitals (p_z and d_{z^2} have been suggested[21]) then these orbitals cannot now overlap efficiently. Indeed, this reinforces the argument that overlap of such orbitals is responsible for the colour change observed in MGS-type salts.

It is interesting to consider whether or not the adoption of the MGS-type structure is dependent on this interaction (weak bond). Yamada[27] has suggested that some electronic effect is involved in the formation of this bond, so that the higher electronegativity of chlorine in $PtC\ell_4^{2-}$ as opposed to bromine in $PtBr_4^{2-}$ causes a weakening of the Pt···Pt bond in the former case and hence destabilization of the MGS structure. There are two obvious factors that control the structure:

(i) Interactions within the chain: These include the Pt···Pt bond as well as repulsions between other atoms. The latter are such that to enable a Pt···Pt approach of ∿3.3 Å the cation must be planar.

(ii) Interactions between chains: These involve the alkyl group of the cations whose size restricts the approach of chains and is also an important factor in packing. The larger the alkyl group, especially when the cation is planar, the greater the packing problem i.e. when the 'spaces' (marked X in the figure below) between alkyl groups become

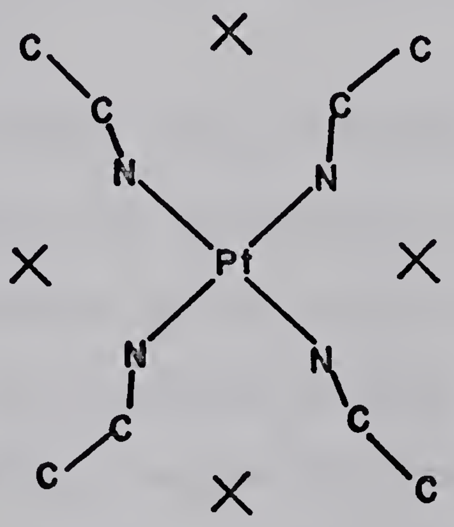

too large to be efficiently occupied by the anions, PtX_4^{2-}, the MGS structure may become unstable.

Presumably then, a balance exists between the stability conferred by the Pt···Pt bond and the instability arising from the packing problem which results because of the necessity to have a planar cation. If in fact the Pt···Pt bond is weaker with $PtC\ell_4^{2-}$, it may be sufficient to exceed the balance point and so destabilize the MGS-type structure. Alternatively the adoption of the MGS structure may be independent of the strength of the Pt···Pt bond so that stability in the packing of the ions is important. Therefore by consideration of its size alone, $PtC\ell_4^{2-}$ would be less successful than $PtBr_4^{2-}$ in filling the spaces (marked X in figure above) and stabilizing the MGS structure. Obviously no choice can be made between the two possibilities namely:

(i) that packing and the metal-metal bond influence the structure, or

(ii) that packing alone is the controlling factor,

without knowledge of the true nature and strength of the bond and the effect on it of changing from bromine to chlorine. Unfortunately there appears to be little agreement in the literature on the true nature and importance of this metal-metal bond.[21,32,33]

The six shortest non-bonding distances,(3.27, 3.34, 3.39, 3.44, 3.43, 3.48)Å , all involve a nitrogen and chlorine atom and are not significantly different from the corresponding distances observed in MGS. Are these sufficiently short, however, to imply hydrogen bonding of the type, $N-H\cdots C\ell$? Several compounds said to contain reasonably strong hydrogen bonding of this type have bond lengths varying in length from 3.10 Å to 3.18 Å with associated infrared N-H stretching frequencies ranging from 3032 cm^{-1} to 2907 cm^{-1}.[30] The comparatively larger bond distances, and N-H stretching vibrations (4 bands between 3135 cm^{-1} and 3240 cm^{-1}) observed in this compound indicate there is no strong hydrogen bonding.

The two independent platinum-chlorine bond lengths 2.33(1) and 2.41(4) Å, are not significantly different and agree reasonably well with the sum of the covalent radii (2.31 Å)[9c] for this bond type. Other platinum-chlorine distances reported are 2.34 Å for $[Pt(NH_3)_4][PtC\ell_4]$[19] and 2.32 Å for $K(PtC\ell_3.C_2H_4)H_2O$.[31] The average platinum-nitrogen distance of 2.09 Å is similar to that found in $[Pt(NH_3)_4][PtC\ell_4]$ of 2.06(3) Å.[19]

REFERENCES

1. E.L. Muetterties and C.M. Wright: Quart. Rev. (London) (1967) 21, 109.
2. R.J. H. Clark, D.L. Kepert, R.S. Nyholm and J. Lewis: Nature (1963) 199, 559.
3. R.J. Gillespie and R.S. Nyholm: Quart. Rev. (London) (1957) 11, 339.
4. D. Britton: Canad. J. Chem. (1963) 41, 1632.
5. Rudolf Kummer and W.A.G. Graham: Inorg. Chem. (1968) 7, 310.
6. M. Elder and D. Hall: to be published.
7. International Tables for X-ray Crystallography (1962) Vol. III Birmingham Kynoch Press, p. 204
8. D.W.J. Cruickshank and W.S. McDonald: Acta Cryst. (1967) 23, 9.
9. L. Pauling; Nature of the Chemical Bond, Cornell University Press (1960) (a) p. 246, (b) p. 260, (c) p. 253.
10. V.A. Semion, Yu. A. Chapouskii, Yu. T. Struchkov and A.N. Nesmeyanov: Chem. Comm. (1968) 666.
11. J.M. Mays and B.P. Dailey: J. Chem. Phys. (1952) 20, 1695.
12. L.L. Merritt and E.D. Schroeder: Acta Cryst. (1956) 9, 801.

13. A.G. Swallow and M.R. Truter: Proc. Roy. Soc. (1962) 266, 527.

14. G.A. Barclay, B.F. Hoskins, C.H.L. Kennard: J. Chem. Soc. (1963), 5691.

15. L.F. Dahl and D.W. Sutton: Inorg. Chem. (1963) 2, 1067.

16. C.H. Wei and L.F. Dahl: Inorg. Chem. (1965) 4, 493.

17. B.G. DeBoer, A. Zalkin, D.H. Templeton: Inorg. Chem. (1968) 7, 2288.

18. F.A. Cotton and G. Wilkinson: Advanced Inorganic Chemistry, John Wiley & Sons (1966) p. 105.

19. M. Atoji, J.W. Richardson, R.E. Rundle: J. Amer. Chem. Soc. (1957) 79, 3017.

20. S. Yamada: J. Amer. Chem. Soc. (1951) 73, 1579.

21. R.E. Rundle: J. Phys. Chem. (1957) 61, 45.

22. J.R. Miller: J. Chem. Soc. (1961) 4452.

23. S. Yamada and R. Tsuchida: Bull. Chem. Soc. Japan (1958) 31, 813.

24. S. Yamada: Bull. Chem. Soc. Japan (1962) 35, 1427.

25. H. Reihlem and E. Flohr: Ber. 67 (1934) 2, 2010.

26. S. Yamada: Nippon Kagaku Zasshi (1965) 86, 753.

27. S. Yamada: Essays in Co-ordination Chemistry, Binkhäuser Verlag, Basel (1964), 140.

28. K. Phillips and D. Hall: to be published.

29. R.C. Strivastava and E.C. Lingafelter: Acta Cryst. (1966) 20, 918.

30. K. Nakamoto, M. Margoshes and R.E. Rundle: J. Am. Chem. Soc. (1955) 77, 6480.

31. J.A. Wunderlich and D.P. Mellor: Acta Cryst. (1954) 7, 130.

32. G. Basu, G.H. Cook and R.L. Belford: Inorg. Chem. (1964) 3, 1361.

33. M.C. Baird: Progress in Inorg. Chem. (1968) 9, 105.

B29919